CEEDWA

2020 CEED SEMINAR PROCEEDINGS

Perth, Western Australia

Monday, September 14th, 2020

Cooperative Education for Enterprise Development

c/- The University of Western Australia

35 Stirling Highway, Crawley, WA, 6009, Australia

CEEDWA

Dr Jeremy Leggoe
Director
Cooperative Education for Enterprise Development

14th September, 2020

Dear Friends

Welcome to the 2020 CEED Seminar, marking the 31st annual celebration of the Cooperative Education for Enterprise Development program. The CEED program staff and scholars thank you for your participation, and trust that you will find your time today well spent.

Many private, public and not-for profit enterprises have achieved significant development through partnering with the CEED program for research projects. The CEED program is designed to provide an efficient way for enterprises to engage with university researchers and students. CEED projects are student research projects undertaken in partnership with public and private enterprises. The project topics are determined by the client enterprise – meaning that CEED projects address real issues in the client's operations, delivering outcomes that enhance performance. The CEED scholars benefit from a unique opportunity to deliver research-based innovation in a real-world environment.

2020 will see the completion of 10 funded projects, and we have commenced an additional 3 funded projects that will continue into 2021. In addition to our funded projects, CEED does offer pro-bono projects for not-for-profit organisations, offering our CEED Scholars the opportunity to undertake research that has an immediate impact in the community. We are also able to welcome CEED Scholars from Curtin University to undertake projects sponsored under the Woodside FutureLab program.

While today's presentations are an important element of the professional development opportunities that the CEED program offers our scholars, we hope that it will also serve to demonstrate the opportunities that the program offers to Client enterprises and the host Universities. The CEED program has completed over 600 projects with more than 90 partner organisations. While the scale of the individual projects may be small, the program has created millions of dollars in research activity, and has produced benefits for our Clients worth many times the initial investments.

For today's celebration we particularly welcome our alumni – the ongoing success of the CEED program is testament to both the contributions that they made when CEED scholars, and the support that they have provided after graduation.

Yours sincerely,

Dr Jeremy Leggoe
CEED Director

A Brief Introduction to CEED

The Cooperative Education for Enterprise Development (CEED) program was founded within the Faculty of Engineering at the University of Western Australia (now the Faculty of Engineering and Mathematical Sciences) in 1989, and now gives access to all disciplines at UWA and Curtin University. The program was based on a model created at RMIT, with initial support via federal and state government funding.

CEED projects are student research projects undertaken for academic credit, most often as Honours, Masters or Engineering Final Year Projects. A new short-term PhD placement model is now available for 2021.

The projects are funded by the clients, and the topics are determined by the client – meaning that CEED projects address real issues in the client's operations or policies, delivering outcomes which enhance performance. Not-for-profit organisations can participate via pro-bono CEED projects.

In most CEED projects, the Scholar spends up to 8 weeks on site with the client during the summer vacation, immersing themselves in the operations and culture of the client while working on their research project. Each CEED Scholar has both an academic supervisor and a mentor from the client enterprise. This ensures that the Scholar remains connected to the client throughout the project, and engages academic staff with the client and the project.

Benefits of CEED projects to client enterprises include:

- Cost effective research projects targeting issues specific to the client.
- Engagement of University experts with client staff and client issues.
- Extended engagement with potential graduate recruits (including the potential to maintain relationships with vacation employees)
- Specialist training of potential graduate recruits in operations and technology unique to the client.
- The opportunity to use the client mentor role in development programs for early career staff.
- Access to University research facilities.

The CEED Team

Dr. Jeremy Leggoe	Director	6488 7315
Ms Amanda Bolt	Administration Officer	6488 3130

Contact Information

Office Phone	08 6488 3130
Office E-mail	ceed@uwa.edu.au
Website	www.ceed.wa.edu.au
Postal Address	CEED Office c/- The University of Western Australia M050 35 Stirling Highway Crawley, WA, 6009

Contents

Automated Livestock Detection and Assistance Technology

Dylan Bedetti

Mohammed Bennamoun
Computer Science
University of Western Australia

Farid Boussaid
Electrical, Electronic and Computer Engineering
University of Western Australia

Jacob Pirone & Anton Wagner
CEED Client: BHP

Abstract

The remote nature of BHP mining operations leads to a number of Light Vehicle (LV) interaction events with livestock. These incidents pose massive risk to both employees and livestock and can be fatal, with two deaths Australia-wide in the last recorded year. Incidents commonly occur during dusk, dawn and at night-time, where there is limited vision and cattle can blend in with their surroundings.

This project proposes a solution comprised of a small Field of View (FoV) thermal camera to feed images to a Convolutional Neural Network (CNN) where computation is completed by the Google Coral, a Tensor Processing Unit (TPU). If the model recognises any livestock, it will alert the user through a speaker. The device has been designed to run 'at the edge' and should operate completely without any internet connection. Early results show promising performance in detecting livestock, especially at critical times such as dusk, dawn and night-time. This research is largely a proof of concept for the technology, which will encourage future development in the area of livestock detection and assistance technology.

1. Introduction

The remote nature of BHP mining operations leads to a number of Light Vehicle (LV) interaction events with livestock. LV's have a gross vehicle mass of up to 4,500 kg and for the purpose of this project is the only vehicle type that will be considered, primarily because they provide the least protection to vehicle occupants in collisions. These incidents can be fatal, with two deaths already Australia-wide in the last recorded year (Australian Associated Motor Insurers, 27), (Government of Western Australia Road Safety Commission, 2016). Incidents commonly occur during dusk, dawn and at night-time, where there is limited vision and cattle can blend in with their surroundings.

Drivers are far more likely to have a collision in regional areas compared to urban areas (Government of Western Australia, 2019). Most of BHP's mine sites operate within 'very remote' areas, which is an index of remoteness derived from the measure of road distance between populated localities and service centres, a term defined by the Australian Department of Infrastructure (Department of Infrastructure, Regional Development and Cities, 2018). These areas have greater than eleven times the rate of road deaths compared to that of major cities (Department of Infrastructure, Regional Development and Cities, 2018), (Australian Institute of Health and Welfare, Rural, regional and remote health - A guide to remoteness classifications). This risk of is amplified further when driving at night time, where limited vision and lack of lighting can decrease a driver's perception and response time, especially for objects that blend in with their background (Green, 2000).

The current controls to avoid LV incidents are limited to the two lowest and least effective methods, Personal Protective Equipment (PPE) and Administrative Controls (AC), shown below in Figure 1. While these controls can mitigate risk of an incident, they are considered minimally effective, and will not eliminate the risk (Australia, 2018).

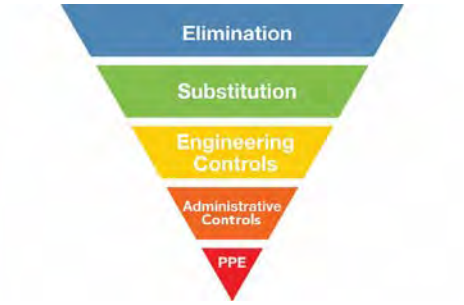

Figure 1 Hierarchy of Controls (Australia, 2018)

The problem of LV livestock collision presents itself as an opportunity to develop a technological risk control through the novel combination of thermal imagery, Deep Learning (DL) and edge computing. To the best of our knowledge, this will be the first research project to date which combines Deep Learning with thermal imagery livestock detection.

2. Process

2.1 Data Collection

Data collection consisted of filming cows on a farm in South-West Western Australia. A normal RGB camera was placed in parallel to the thermal camera to give images a source of ground truth. An output of this is shown in Figure 2 below.

Figure 2 Data collection using RGB and thermal camera

Choosing a thermal camera requires balancing cost and image resolution constraints. The scope of this project limited the cost of the product to a maximum of $3000. Because of this cost restraint, the only thermal cameras available have low image resolution. However, a small FoV camera can provide high pixel density, even at lower resolutions. The thermal camera chosen was an AXIS P1280-E with a horizontal FoV of 35.4°, a resolution of 208 x 156 pixels and a frame rate of 8.3 frames per second (FPS) (AXIS Communications, n.d.).

Figure 3 shows the FoV of the AXIS thermal camera when mounted on a vehicle. The camera can see past the boundaries of the road after 11.5 meters. After 40 meters the camera will show a front-facing cow with 10 pixels, and a sideways facing cow with 30 pixels.

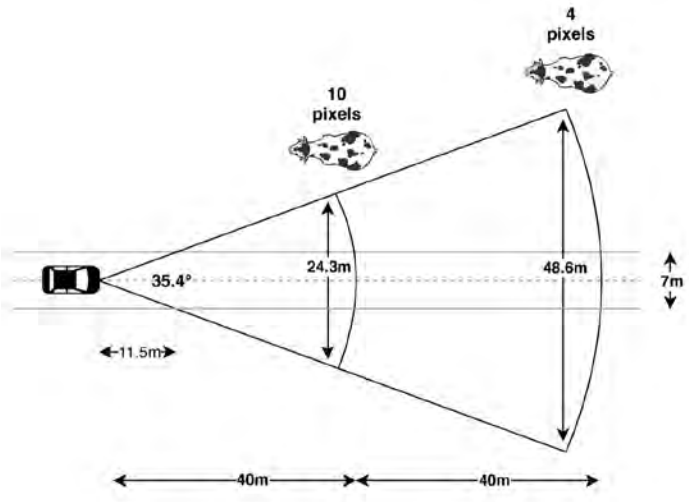

Figure 3 Thermal Camera FoV

2.2 Model Training

A core requirement of the solution is model inference speed, as the faster the inference of the model, the faster a driver can be alerted of cattle ahead. To achieve this speed, the Google Coral (Google, n.d.), an edge compute Tensor Processing Unit (TPU) was used. Currently, the Google Coral only supports MobileNets for detection-based models. The Coral is at the forefront of edge Deep Learning and is still being further developed.

MobileNet Single Shot Detector (SSD) V1 which had been trained on the Common Objects in Context (COCO) dataset was used for transfer learning of the last few layers (COCO, n.d.). The

MobileNet model has input dimensions of 300 x 300 pixels which required resizing of the thermal camera image from 208 x 156 pixels. The tensor required for training of the MobileNet model has 3 input channels, however the thermal image only returns a single channel of thermal intensity. It was therefore decided to duplicate three copies of the thermal image to get the desired number of channels.

A thousand images were chosen from the data collection and were labelled. These were used for training with an 80/20 split for training and testing data. The model was only trained with a single class of 'cow'. Most of the convolutional layers were frozen, with only the last few pointwise and depthwise convolutions remaining unfrozen, and malleable during training. The training was completed with 500 training steps and 100 evaluation steps. Further training did not significantly increase model performance.

Google also offers an Automatic Machine Learning (AutoML) service, which only requires a training dataset and object labels. The AutoML service will test multiple different model architectures and attempt hyperparameter optimisation on each with the goal of returning the best model for the given input data.

The same dataset of 1000 images and labels was fed into the Google AutoML service. The resulting model achieved a precision of 93.77% and a recall of 59.32% at an IoU and confidence threshold of 50%.

3. Results and Discussion

The MobileNet Edge TPU enabled model was chosen for the MVP over the AutoML model because of the smaller number of model operations, 64 compared to 294, and the greater percentage of Edge TPU enabled operations, 98% compared to 45%.

For the application of this product, speed is more important than accuracy. This is because the possible impact of a false positive has less risk than a false negative. Also, the risk of a collision grows as the delay between capturing an image and alerting the driver increases. Therefore, for this product, a model that achieves fast inference with less accuracy is preferred over one that has slow inference but higher accuracy. Figure 4 below illustrates the model's ability to detect cows within the test dataset.

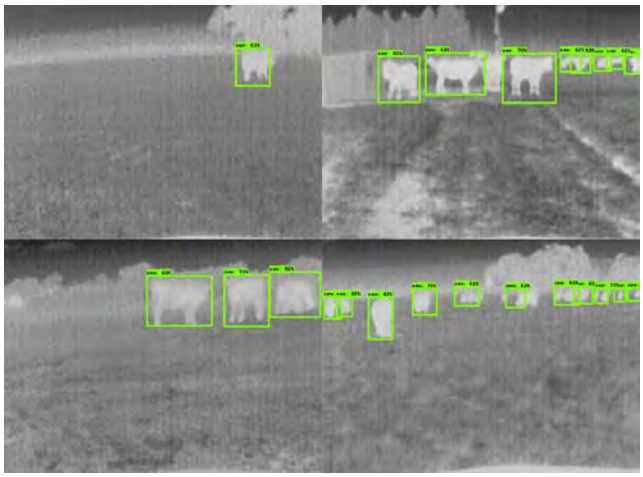

Figure 4 Model detections on testing data

The associated weighted sigmoid focal loss, plotted in Figure 5, indicates the presence of a learning process. However, after testing the inference with live field data, it became evident that the model is not accurate in distinguishing different objects with similar thermal signatures, such as being able to differentiate a cow from either a human or car at distance.

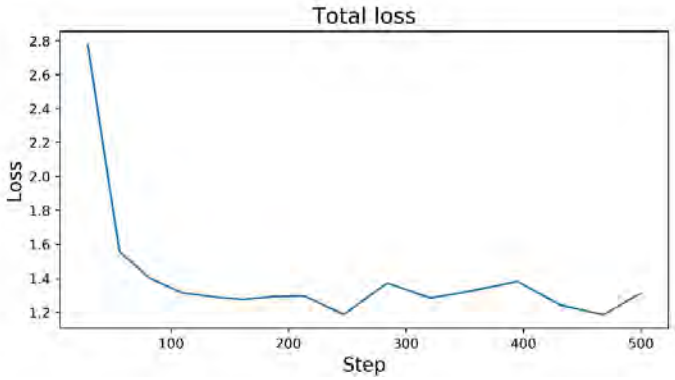

Figure 5 Weighted sigmoid focal loss

This limitation is likely caused by the thermal camera resolution, as at a distance of 40 meters, an object the same size of a forward facing cow will be visible in only 10 pixels of the image (AXIS Communications, n.d.). All visual Deep Learning methods are restricted on using the information available in the image presented, and the information that can be conveyed by 6 pixels in a grayscale image is limited.

4. Conclusions and Future Work

An MVP has been successfully developed, tested and evaluated in and around a BHP mine-site environment for detecting and alerting the presence of cattle. This project was sponsored by BHP, in-partnership with UWA and was supported by many individuals throughout both organisations.

The product delivered is a cattle detection retrofit kit for LV's which uses a combination of GPS position and a Deep Learning model for inference and alerting drivers. The project offers a scalable software platform and recommended technical direction for further development.

Such a project is made possible with the very recent advances in hardware, software and Deep Learning. It is truly exciting to imagine what impact these technologies will have in the coming years as they become faster, smaller and more integrated. It is the hope of the author that this project can be used as both a stepping stone for further development and as inspiration for others to pursue improvement and change through technology.

5. Acknowledgements

I would like to express my sincere gratitude to everyone who supported, challenged and educated me during my final year thesis project. To the University of Western Australia who provided me with the opportunity to pursue a Masters degree in Professional Engineering, and for giving me the tools to succeed. To the Co-operative Education for Enterprise Development program, Jeremy Leggoe & Amanda Bolt for providing me with the opportunity to undertake an industry focused Thesis and for the ongoing support and guidance. To BHP, Jacob Pirone & Anton Wagner for enthusiastically accepting my project proposal, continuing my professional development and for guiding me through the challenging process of building, innovating and

developing.To Winthrop Prof. Mohammed Bennamoun & Prof. Farid Boussaid for providing me with technical insight and inspiration, and for furthering my education and passion of machine learning.

6. References

Australia, S. W. (2018). *How to manage work health and safety risks.* Canberra: Safe Work Australia.

Australian Associated Motor Insurers. (27, 5 27). *AAMI animal car accidents data 2019*. (AAMI) Retrieved 8 28, 2019, from https://www.aami.com.au/aami-answers/insurancey/aami-reveals-peak-periods-for-animal-collisions.html

Australian Institute of Health and Welfare. (Rural, regional and remote health - A guide to remoteness classifications). *Australian Institute of Health and Welfare.* Canberra.

AXIS Communications. (n.d.). *AXIS P1280-E Thermal Network Camera*. (AXIS) Retrieved May 3, 2020, from https://www.axis.com/en-au/products/axis-p1280e

BHP. (2019). BHP Event Reporting Portal (ERP). Perth: BHP.

BHP. (2019). Light Vehicle Collision with Livestock at Blackwater Mine. Brisbane: BHP.

COCO. (n.d.). *Common Objects in Context*. Retrieved May 2, 2020, from http://cocodataset.org/#home

Department of Infrastructure, Regional Development and Cities. (2018). *International road safety comparisons 2016.* Canberra.

Google. (n.d.). *Coral*. Retrieved May 2, 2020, from https://coral.ai/

Government of Western Australia. (2019). *2018 Preliminary summary of fatalities of Western Australian roads.* Perth: Road Safety Commision.

Government of Western Australia Road Safety Commision. (2016). *Reported road crashes in Western Australia 2015.* Perth: Road Safety Commision.

Green, M. (2000). "How Long Does It Take to Stop?" Methodological Analysis of Driver Perception-Brake Times. *Transportation Human Factors, 2*, 195-216.

Loughnan, L. (2011). FENCING ROAD RESERVE IN PASTORAL REGIONS MAIN ROADS/PGA & STAKEHOLDERS . Perth: Main Roads Western Australia .

Mainroads Western Australia. (2019, May 8). *Design of Fencing/Walls*. (The Government of Western Australia) Retrieved September 7, 2019, from https://www.mainroads.wa.gov.au/BuildingRoads/StandardsTechnical/RoadandTrafficEngineering/RoadsideItems/Pages/Design_of_Fencing_Walls.aspx

Rebecca Butcher, S. C. (2019, Feburary 13). *The Western Australian beef industry*. (Department of Pimary Industries and Regional Development) Retrieved September 7, 2019, from https://www.agric.wa.gov.au/industry-development/western-australian-beef-industry?nopaging=1

WALGA. (2017). *Reference information for Elected Members on a Regional Road Group.* Perth: Pilbara Regional Road Group.

Development of Robotic Methods for Accessing Marine Piles

Samuel Tennent

Thomas Braunl
Electrical, Electronic and Computer Engineering
The University of Western Australia

John Forlani
KAEFER Integrated Services Pty Ltd

Abstract

Currently jetty piles can only be accessed through either rope access, divers or often both. These methods require significant safety apparatus and are slow, manpower intensive activities. Precise work is difficult due to the low stability of the work environment. KAEFER Integrated Services in collaboration with UWA is developing a robotic platform to more efficiently access these areas and remotely conduct works. This will ensure the processes are conducted much more reliably and precisely whilst increasing speed and accuracy. This novel approach will require new robotic technologies and methods to operate in these environments. Some examples of these new technologies include digital fabrication via 3d printing, low cost micro-controllers and more. As well as these operating advantages, the ability to remotely access equipment and monitor it is becoming more in demand as companies seek to further digitally integrate processes on work sites. A robotic solution will significantly improve work process in this traditionally difficult and hazardous role.

1. Introduction

1.1. Background

Piles are the structural element that support all marine structures. The marine environment creates significant challenges, mainly marine growth and surface corrosion (Arafati, Hossein, Mousavi, Rouzmehr, 2012). Both of these effects mean structures must be cleaned, inspected and then either wrapped or painted at regular intervals in their life span (Department of Defence United States of America, 2012). While these functions are fairly non-technical and straightforward to perform on land, many challenges are added in the marine environment. Accessing piles to perform these actions generally involves using a combination of rope access, boats or divers (EtherNDE, n.d.)(GeoVert, n.d.). These specialised methods make pile maintenance significantly more challenging than land based structural maintenance.

There have been significant advances in robotic technology in recent years. Consumer devices such as smartphones and drones have resulted in a reduction in the cost of micro-computing technology and electromechanical components (Abhishek, Keshav, Gautham, Samuel, 2017). Manufacturing of custom mechanisms has been advanced with the proliferation of digital fabrication methods such as 3D printing, laser cutting and CNC milling (M. Lau, J. Mitani and T. Igarashi, 2012)(Stansell, Tyler-Wood, 2016). Lastly, new computational methods such as convolutional neural networks have meant that lower cost cameras can be used to access a

robot's environment in ways that previously required more expensive sensors (Krizhevsky, Sutskever, Hinton, 2017). All of these factors have resulted in a wave of robotic solutions for industry challenges.

1.2. Problem Statement

By their nature, rope access or using divers and boats are not effective solutions. Divers and Rope Access Technicians are highly skilled workers and thus are highly paid workers. Their labour costs can often be the largest cost in a project. In the environment they struggle to provide a stable platform for precise works. This results in precise work often being done slowly. The human nature of their work means that works may be performed inconsistently between piles. Thus the current methods of accessing marine structures can be described as inconsistent, slow and imprecise. Therefore lower cost and faster technologies to access and operate on these piles are needed.

1.3. Industry Benefit

It is the intention of this research to apply low-cost modern robotic methods to a traditional labour problem. Robots are able to conduct works much more precisely than human workers. This precision means that maintenance standards can be achieved more consistently. As well as consistency, the robotic solution operates faster than a comparable human solution and achieves significantly reduced labour costs for companies. These benefits have traditionally came at a high cost both in designing time and component cost, prohibiting their development. However, this research wishes to utilise new modern robotic methods while achieving a reduction in cost of parts and processes.

2. Process

2.1. Overall

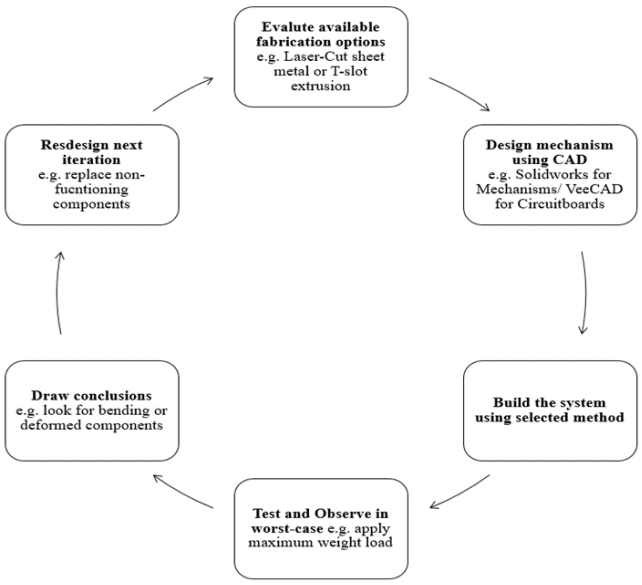

Figure 1 Simple system prototype process

The prepared robot, like most robots, is ultimately a combination of simple mechanisms and systems. The design of these systems has followed a simple cycle, illustrated in figure 1. Ultimately, once all of these systems have been prototyped to an acceptable standard, they are combined to first test if they function together, and then tested to their limits to determine their performance.

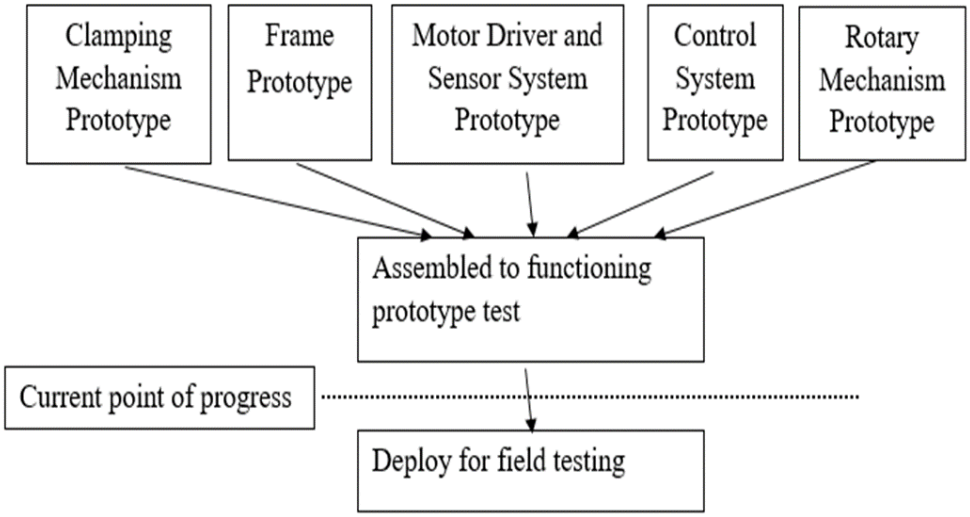

Figure 2 Overall Prototype Process

2.2. Tools, Equipment and Methods

Design Tools

- Solidworks for Component CAD (Solidworks Education, 2020)
- Solidworks for FEA Analysis
- VeeCAD for circuit board design (VeeCAD, n.d.)

Fabrication Tools

- 254cm 80T MitreSaw for aluminium cutting
- 1200W Laser Cutter for steel sheet cutting
- Metal Bender for sheet metal bending
- BenchTop 2kW Mill for small aluminium milling
- CNC 3-Axis Router for large section or custom-shape aluminium
- CO2 Laser Cutter for platic cutting
- Cordless drills for bolted component assembly
- Cordless angle grinder for metal deburring
- Soldering iron station for circuit board assembly

Software/Firmware Tools

- Arduino IDE for firmware coding and flashing (Arduino, n.d.)
- VisualStudio Code for C++ and Python programming
- Python 3.7 for High Level Software (Python Licensing, n.d.)

3. Results and Discussion

To date the results of the research have been delivered through tests in the form of prototypes and analysis.

Test	Date	Observation	Discussion
First Clamp Prototype	21st May 2020	• Inconsistent climbing speed • Clamping Actuator not holding	• Stronger Actuators needed • Stiffer Rails needed
Second Clamp Prototype	16th July 2020	• Despite >100kg direct loading in multiple directions, mechanism works fine • Some hinges broke during assembly	• Hinges to be redesigned or procured
First assembled Test	23rd July 2020	• Signifigant flexing and deformation of the frame • Difficult to climb under manual control	• Larger frame using thicker aluminium extrusion and wider steel bracing • Control algorithm will have to synchronize all mechanisms
Second Frame FEA Analysis	3rd August 2020	• ~90% less deformation under simple FEA analysis not including all bolt holes in analysis	• Second frame design will likely be effective

Table 1 Prototype and Finite Element Analysis tests

4. Conclusions and Future Works

4.1 Conclusions

Based on the results, it has been determined that, despite failures of some specific components during prototype tests, overall the concepts used in the mechanisms designs and prototypes are sound. At this stage it is likely that the research will successfully yield a robot with the desired outcomes.

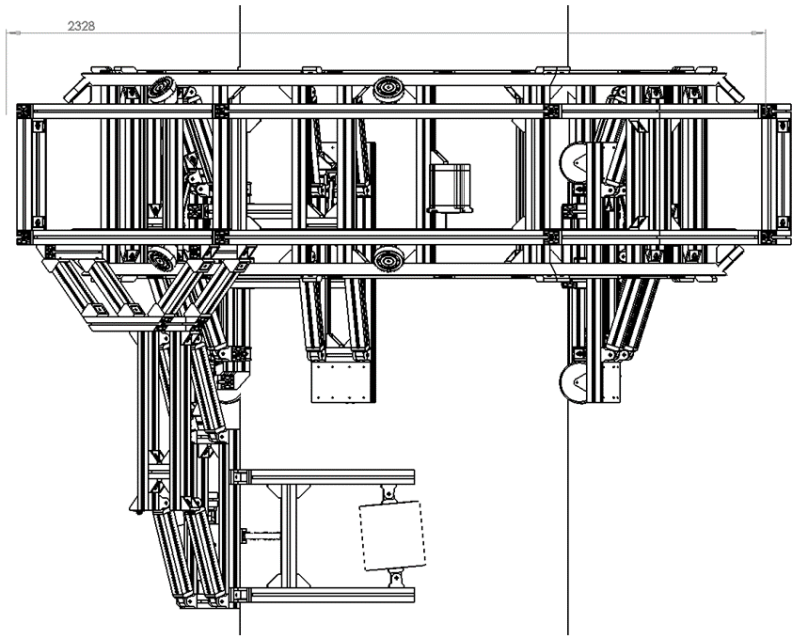

Figure 3 Prototype Design

4.2 Future Works

Modular Attatchments
Clearly, once the robot is completed it will need to be able perform actual works. Thus, the modular attachments to enable it to do so will be needed. These will most likely include an Airless paint gun for painting, pneumatic bristler for blasting, and surface finish and X-Ray Mount for inspection.

Automatated Components
Despite being less labour intensive than traditional methods, the robot still requires multiple skilled operators in its current configuration. This is because some of the mechanisms, such as its locking mechanism require manual operation in set up. It is the goal that by automating these operations, the robot further reduce labour costs.

Performance enhancements
The robot being developed by this project is intended to be fully functional, however as the robot operates in the field, it will become much clearer which components are very effective and which need to be further optimized or replaced. This will likely result in further versions which may be lighter or faster and more rugged due to replaced higher-quality or better designed components.

5. Acknowledgements

KAEFER Integrated Services
KAEFER has been instrumental in providing not only the funding but also the faciltiles for the majority of the fabrication to take place. Special mention to John Forlani for mentoring the project as well as Chris Rawlinson and Glenn Coles for assisting with fabrication and providing useful design advice.

Thomas Braunl
Prof. Braunl has been very helpful not only supervising the project but also in his teaching of the *Robotics* and *Embeded Systems* units, which provided fundamental learnings in order for this project to be possible.

UWA CEED Office
CEED has done a great job in providing a facility for all of the available stakeholders to participate and the experience has been invaluable for all involved.

UWA Makers
A special mention has been attributed to UWA Makers Club, which has not only provided excellent electronics and laser cutting facilities, but has also provided a rare facility for the basic training of small skills like soldering which are essential for any robotics project.

7. References

Arduino, n.d. (https://www.arduino.cc/en/main/FAQ)

B. Abhishek, K. Keshav, S. Gautham, D. V. R. R. Samuel and S. R. Nair, "Low cost ROS based semi-autonomous drone with position and altitude lock," 2017 IEEE International Conference on Power, Control, Signals and Instrumentation Engineering (ICPCSI), Chennai, 2017, pp. 2109-2112.

EtherNDE, Application Notes: Pulsed Eddy Current Inspection of Jetty Piles, n.d. (http://www.andesb.com/assets/maxwell-jetty-pile.pdf)

GeoVert, Red Mud Marine Pipeline Marine Pipeline Maintenance and Corrosion MANAGEMENT, n.d.(https://assets.ctfassets.net/sc89kfcx318h/7I4hvusdHyMoiAAISOYckC/be6c2a02f5d71358255d6a1f85ae31ae/Red-Mud-Marine-Pipeline-PP.pdf

Glassdoor.com.au Rope Access Salary, n.d., https://www.glassdoor.com.au/Salaries/rope-access-salary-SRCH_KO0,11.htm)

IAS Group Diverless Sitejacket Steel Pile Strengthening & Protection, n.d., http://www.ias-group.com.au/view/case-study-articles/5-sitejacket-structural-steel-pile-strengthening-and-protection-in-splash-zone

KAEFER Integrated Services Coatings, n.d., https://www.kaefer.com.au/Surface-Protection/Coatings.html)

KAEFER Integrated Services Linings, n.d., https://www.kaefer.com.au/Surface-Protection/Linings.html

Krizhevsky, Alex; Sutskever, Ilya; Hinton, Geoffrey E. (2017-05-24). "ImageNet classification with deep convolutional neural networks". Communications of the ACM. ISSN 0001-0782.

Python Licensing, n.d. (https://docs.python.org/3/license.html)

Solidworks Education, 2020,https://www.solidworks.com/sw/education/6903_ENU_HTML.htm

VeeCAD, n.d., https://veecad.com/about.html

A Study on Gross Pollutant traps in Drainage Channels

Giorgia De Bellis

Anas Ghadouani and Liah Coggins
Civil, Environmental and Mining Engineering
The University of Western Australia

Paola Duarte Romero and Jason MacKay
CEED Client: Water Corporation

Abstract

Despite the wide implementation in Australia of Gross Pollutant Traps (GPTs) in local drainage systems, there is limited understanding of their performance and operational requirements. The purpose of this study is to review the available information on the performance and operational requirements of the devices of interest (drainage nets, floating booms and floating traps) through a literature review and consultation with different stakeholders and to standardise a monitoring methodology for the nets based on the current maintenance methodology undertaken by the City of Kwinana. The high frequency of the City of Kwinana's drainage nets inspection and cleaning ensures that the units are efficient at each storm event but additional data would be beneficial to develop a common basis for comparing trap performance.

1. Introduction

During a rainfall event large enough to generate runoff across the surface, accumulated pollutants on urban impervious surfaces may be quickly mobilized by stormwater runoff and discharged into receiving waterways. Gross pollutant traps (GPTs) are a tool to reduce litter and debris being transported in drains. These devices are installed in drainage infrastructure to capture and retain gross pollutants (litter and organic debris greater than 5 mm) by physical screening.

Water Corporation is investigating measures to reduce the level of plastic waste in stormwater discharge to the ocean, as part of its commitment to the State Waste Strategy Action 1.14, and proposes to run a trial installing Gross Pollutant Traps (GPTs) in Herdsman Lake's drainage system. The trial seeks to determine the investment, in terms of life cycle cost and operational and assess the effectiveness of two different types of GPTs. Initially, the GPTs considered as possible options included drainage nets (Figure 1a), floating litter booms (Figure 1b) and floating litter traps (Figure 1c). The net were found unsuitable to install in Herdsman Lake due to the required size of these nets to service the existing pipes, plus the operational and wildlife protection challenges. The Corporation continues to investigate the possibility of installing a trash net(s) in a suitable drainage outlet. Despite the wide implementation of GPTs in local drainage systems in Australia there is little evaluation of their performance in arterial drainage systems, and limited evaluation of their trapping efficiency and operational requirements (Wong et al, 1999).

This study is part of the broader project to install GPTs in Herdsman Lake's drainage system and will assist the Corporation to determine the performance and the economic burden of the selected GPTS and to assess the possibility to broaden their use in the Corporation's drainage network. The project aims to achieve the following objectives:

- Develop an understanding via a literature review of the performance, maintenance and operational requirements of drainage nets, floating litter booms and floating litter traps providing a point of comparison to the actual data that will be collected once the Herdsman Lake GPTs are installed.
- Standardise a feasible, cost-effective methodology for monitoring drainage nets based on the current maintenance methodology undertaken by the City of Kwinana.

Figure 1 GPTs of interest: (a) drainage net, (b) floating litter boom, (c) floating litter trap.

2. Process

2.1 Literature Review and Consultation with Stakeholders

The first objective of the project is to undertake a literature review of previous studies and reports on drainage nets, floating litter booms and floating litter traps and to consult with different stakeholders such as local governments, water utilities and suppliers to collect data on performance, operation activities, costs and monitoring methodologies of the GPTs of interest.

2.2 Analysis and Optimisation of the City of Kwinana's Monitoring Methodology

The knowledge acquired through the literature review and consultation with stakeholders establishes a starting point to standardising a monitoring methodology for the drainage nets. The City of Kwinana consented to collaborate on this project by allowing their nets monitoring methodology to be used as a case study for the optimization and/or standarisation of a

monitoring methodology. The following steps are necessary for identifying gaps, determing if and how they could be improved and for capturing any lessons learnt:

- *Analysis of Current Monitoring Methodology* involves a discussion with the City about the drivers behind the nets installation and the maintenance and monitoring activities. This analysis aims to assess the effectiveness of: 1. the devices, 2. the frequency of maintenance and inspection, 3. the cleaning method and costs, 4. the equipment employed and personnel involved and 5. the waste disposal procedures.
- *Catchment Characterisation* and its visual survey aim to investigate the catchment's stormwater pathway, the critical gross pollutants sources and site constraints through a visual survey and a desktop assessment of the catchment. The catchment characterization include assessing:
    - catchment size, land use and site constraints,
    - collection of information on nature and hydraulics of the drains (pipe and open drain locations, dimensions and lengths),
    - key maintenance activities within the catchment that may affect gross pollutant loads (street sweeping, waste removal services, local drainage maintenance),
    - identification of potential sources of gross pollutants through review of available land use planning information and aerial photography to identify key land uses that source gross pollutants.

3. Results and Discussion

3.1 Literature Review and Consultation with Stakeholders

From an analysis of previous reports emerged the general lack of data collected on GPTs and specifically about those designs that are considered in this study. Despite several GPTs installations across the country, very few local authorities collect extensive and detailed data about their GPTs. The performance data are available in the form of the weight or volume of gross pollutants removed from the traps, but the lack of other meaningful data such as gross pollutants not captured by the unit, catchment area, rainfall and water levels data doesn't allow the development of a common basis for comparing the capture efficiency of different waste interception devices (Wong et al., 1999).

As part of the literature review, 60 stakeholders were consulted across Australia including local governments, water utilities and suppliers and the main findings of this process are summarized in Table 1. Their responses varied greatly in term of GPTs' efficiency and maintenance method and this variance could indicate that the devices are actually operating at various degrees of performance, as already reported by a CSIRO's review (Neumann & Sharma, 2010). The effectiveness of a GPT is not only defined by its design but is also strictly dependant on its individual maintenance and operational actions. Because these factors are impacted by budget, site accessibility, catchment characteristics and gross pollutant load in the catchment, it is important to adjust monitoring activities and schedule to the specific catchment and location on a case by case basis (Wong et al, 1999). The devices of interest in this review require regular and frequent maintenance in order to prevent problems such as water quality issues, sediment buildup, performance decline and deterioration of the structure itself. To this end, standard procedures in assessing and reporting the system's efficiency and in scheduling and reporting maintenance activities would ease the management requirements of these units.

	Drainage nets	Floating litter booms and traps
Performance	Capture efficiency of gross pollutant around 90% Performance is catchment specific. Less efficient the bigger the pipe	Capture efficiency of floating pollutants ranging from 12% to 50% Efficiency is rainfall and water-depth dependant
Main issues	Water quality issues	During high flows trapped material may escape
Maintenance frequency	Varies from 'every 6 months' to 'twice per month'	Varies from 'monthly' to 'weekly'
Inspection frequency	Varies from 'every 6 months' to 'after every heavy rain'	Varies from 'monthly' to 'after every heavy rain'
Equipment	Front-end loader and tipper truck Boom truck crane	Excavator or vacuum truck Manually with a pool scoop Skimmer vessel

Table 1 Summary of the results of the literature review and consultations with local authorities

3.2 Analysis of the City of Kwinana's Monitoring Methodology

The City of Kwinana reported one of the most efficient method in managing the drainage nets which represents a valuable basis for the development of a standard monitoring methodology for the nets. The City has five drainage nets in their drainage system. The first 2 nets were installed in 2018 and additional three nets were installed in 2020 (Table 2). The installation of drainage nets and GPTs is one of the actions outlined in the City's Sustainable Water Management Plan to address the litter impact on water quality of stormwater and to improve ecological health and ensure quality urban space (City of Kwinana, 2018).

The Council maintains the drainage nets through in-house personnel and equipment. As part of the monitoring activities, they developed a Safe Work Instruction for handling the nets and dedicated training course for the personnel involved. The City did not attempt to assess the effectiveness of the devices but from an analysis of the nets' maintenance data (Table 2) it can be concluded that there are variations in gross pollutant loads due to different catchment characteristics. Based on visual observations, the waste is made up mostly by organic matter and a minimal percentage (10%) of litter such as plastic bottles and cans. Additional data in their maintenance sheets related to catchment area, rainfall and water levels data would be helpful to be collected to develop a deeper understanding of nets performance.

The City proved being actively committed to improve the nets maintenance method, as shown in Table 3, by halving the required time to clean the nets from two hours to just one per device. In this way, they reduced the cleaning cycle cost per device from $304 to $152. The high frequency of the City of Kwinana's inspection and cleaning of their devices ensures that the unit trapping efficiency is optimum for each storm event and that materials do not decompose or stagnate causing water quality problems.

Locations of the Nets	Installation Year	Waste Collected in 2018 (kg)	Waste Collected in 2019 (kg)	Waste Collected in 2020 (kg)	Total
Site A	2018	670	892	395	1957
Site B	2018	260	147	90	497
Site C	2020			172	172
Site D	2020			60	60
Site E	2020			155	155

Table 2 Waste collected from the different locations of the nets since their installation. The data of 2020 refer to the waste that has been collected in 7 months (until July 2020) .

Item	2018	2019
Inspection frequency	After heavy rainfall	After heavy rainfall
Maintenance frequency	Wet Season: Twice per month Dry Season: Every 2 months	Wet Season: Twice per month Dry Season: Every 3 months
Annual Cleaning Cycles	8	6
Equipment and staff required	Front end loader, Tipper truck Two Officers	Front end loader, Tipper truck Two Officers
Time to clean 1 drainage net	2 hours (Each officer)	1 hour (Each officer)
Cost to clean 1 drainage net	$304	$152
Vandalism cost	$220	$220
Waste disposal cost/tonne	$80	$80

Table 3 Maintenance method, frequency and costs of the nets of the City of Kwinana from 2018 to 2019.

3.3 Site E's Catchment Characterisation (City of Kwinana)

The selected location at which to undertake a catchment characterisation is a drainage net installed in 2020 at Site E. The unit is located on the north-east perimeter of a park, draining a predominantly residential zoned R12.5/20 and commercial sub-catchment (Figure 2). The catchment covers an area of approximately 140 ha and the potential gross pollutant sources include pharmacy shop, takeaway food outlet, grocery shop, and liquor store. Based on an analysis of the waste collected in the net during the last seven months, the catchment contributed 1.11 kg per hectare of gross pollutants.

There are approximately 550 m of City of Kwinana's drainage network between the top end of the catchment and its discharge point. Side entry pits and grated pits are the primary types of pits seen within the catchment area. The information on the drainage system in the catchment derives from historical data and part of its hydraulic information is missing which doesn't allow a hydraulic analysis of the system to be undertaken.

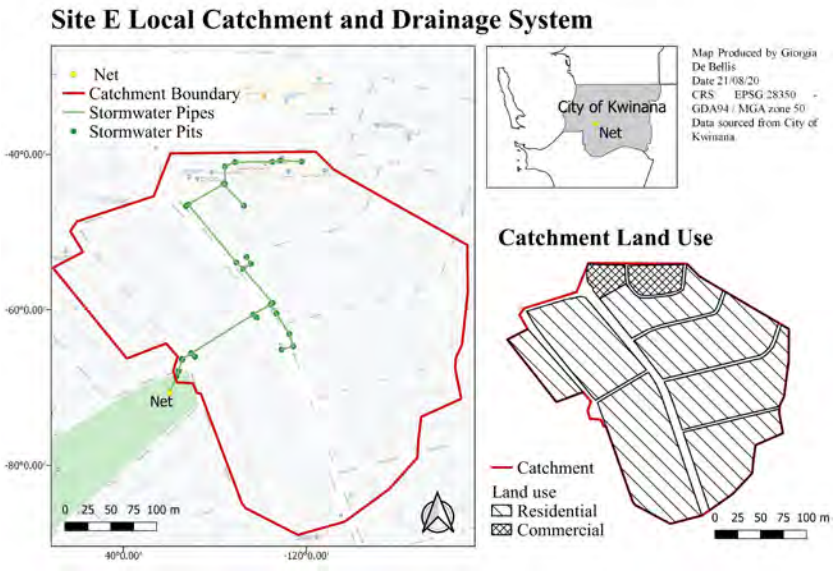

Figure 2 Site E Catchment identification and Drainage system.

4. Conclusions and Future Work

The drainage nets effectively address the litter problem the City of Kwinana has in its bush reserves because of the effective and frequent maintenance the City performs on their devices. Additionally, the selected drain outlets were highly suitable for the nets given that the discharge basins are mostly dry systems with ease of access for maintenance vehicles.

The remaining work of this study will endeavor to optimise/standarise the City's monitoring methodology based on the findings of this analysis. It is advisable to test the benefits of the proposed process by applying it to other local governments GPTs locations. It is also recommended to study the impacts of these GPTs on water quality and hydraulics to fully understand the implications of these devices and guide informed future decisions on their use and applications.

5. Acknowledgements

I would like to recognize the inestimable assistance and enormous support of my Water Corporation mentor Paola Duarte Romero, without whom I would not have made it through this research. Thanks to my supervisor Anas Ghadouani for believing in me and always supporting me. My deepest gratitude to my mentor Jason MacKay and to Suzanne Brown, Amanda Best and the rest of the Drainage and Liveable Communities team for embodying the essence of the One Team value. I am grateful to the City of Kwinana for their collaboration in this project, particularly Kim Logue for her time and help.

6. References

City of Kwinana. (2018). Sustainable Water Management Plan. City of Kwinana.

Neumann, L. N., & Sharma, A. (2010). Literature Review on Performance Testing Approaches for Gross Pollutant Traps. CSIRO: Water for a Healthy Country National Research Flagship.

Wong, T., Wootton, R., Argue, J., & Pezzaniti, D. (1999). Bringing Order to the Pollution Control Industry: issues in assessing the performance of gross pollutant traps. The Int. Congress on Local Government Engineering and Public Works, CE42, pp. 1-8. Sydney NSW Australia.

Detection of Ragging in Wastewater Pumps using Condition Monitoring

Amitkumar Patel

Melinda Hodkiewicz & Adriano Polpo
Mechanical Engineering
University of Western Australia

Craig Hay & Benjamin Chan
Perth Region Field Services
Water Corporation

Abstract

The unexpected blockage of wastewater (WW) pumps caused by debris in wastewater is an ongoing challenge managed by the Water Corporation (WC). Removing rags and restoring pumps to service incurs significant labour costs and a risk of safety exposure because of the need to undertake entry to confined spaces to access dry well pumps. Ragging impedes pump performance and can result in damage to the pump's internal components. Currently there is no accepted method to predict ragging. This paper assesses the suitability of vibration and motor current for ragging event prediction. Vibration and pump motor current data were collected on 7 small WW pumps (<10 kW) in 6 different pump stations over 3 months. The set data includes 16 ragging events. Findings suggest that an increase in motor current is a reliable indicator of ragging. The vibration response of pumps to ragging is not consistent and it does not appear to be a reliable indicator. Preliminary statistical analysis suggests that motor current alone should be used for these small pumps and the additional costs involved in vibration data collection are not warranted.

1. Introduction

Water Corporation's wastewater network has 1,234 wastewater pump stations (817 Metro and 417 Regional) which operate to transfer wastewater collected from end-users via a network of gravity sewers to Wastewater Treatment Plants (WWTP) for treatment and eventual discharge to the ocean. The WWPS deals with both domestic and industrial waste entering the network and absorbs a variety of waste including foreign objects which have the potential to damage or clog (rag) the wastewater pumps. Wastewater pumps are designed to transfer wastewater however based on WWPS design, pump specifications, impeller types and flow rate some pumps are more susceptible to ragging than others. Ragging is a functional failure of the pump due to accumulation of debris in WW pumps and various other factors explained in the study done in Water Corporation (Marinko, 2018). De-ragging is a reactive maintenance activity which always requires a team of technicians to be on standby to attend the site and clean the pumps in the event of an occurrence. Additionally, partial ragging of larger pumps results in increased energy consumption and if left unchecked, could reduce the pump life due to operating off Best Efficiency Point (BEP).

WWPSs are monitored through SCADA and Ademco communication systems at the Water Corporation Operations Centre (OC). Various measurement techniques (current, power, flow)

to monitor pump performance are used by the Water Corporation, however this data is not currently used proactively to identify potential ragging events. Typically, ragging events are indicated by the activation of standby latch alarms. These are triggered when the pump cannot keep up with inflow and the wet well level reaches "Standby Alarm" level. This alarm triggers the control system to shut the operating pump down and start the second pump. Irrespective of the fault type, the OC will then call out the duty electrician to attend site to check the fault and identify the problem. If pump clogging is confirmed, additional mechanical team resources will attend site to perform a pump de-rag.

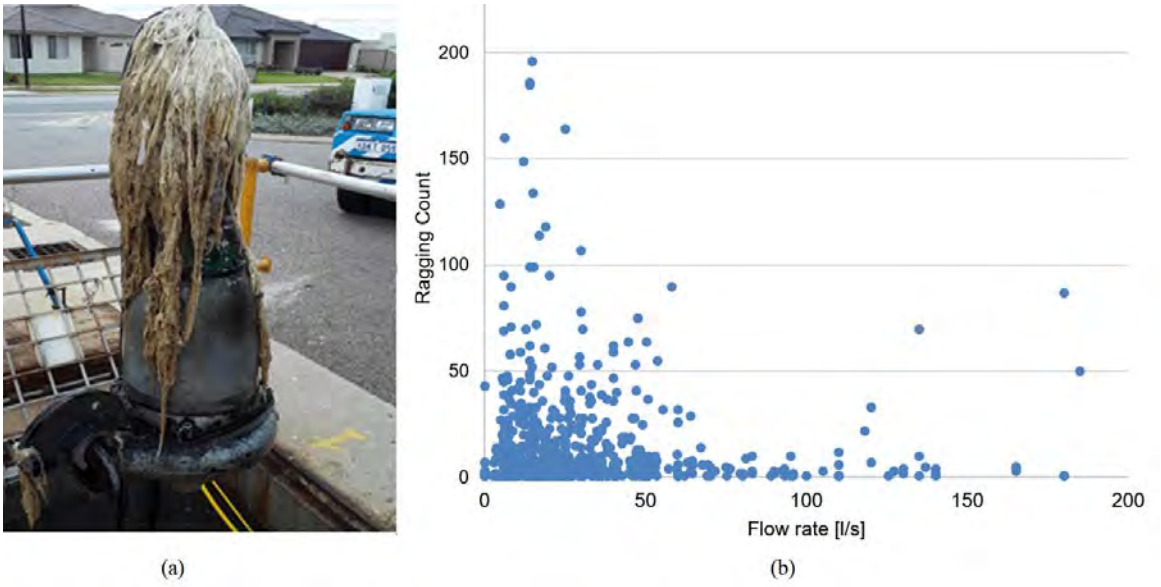

Figure 1 Rags caught on pump body at a WWPS, Perth shown in (a). Ragging count from January 2016 to December 2019 shown in (b) where each dot represents a WWPS.

Figure 1(a) shows an example of the amount of debris caught on a pump body during a de-rag activity. Responding to these events is an around-the-clock requirement. Ragging events occur in all three types of WWPS designs: Dry well, Wet well and Vacuum WWPS. Historical data analysis of ragging history of all WWPSs from 2016 to 2019 was conducted to understand ragging frequency and identify candidate pumps for data collection. A plot of ragging counts vs pump flow rate (a proxy for size) is shown in Figure 1 (b). The diagram shows that smaller pumps have a much higher count than larger pumps with some WWPSs having over 150 events in the 4 years. The six most frequently ragging dry well stations were chosen to be a part of this project. All have a motor size of less than 10 kW and flow rate of less than 20 L/s.

1.1 Motivation

The objective of this project is to assess the suitability of two condition monitoring techniques, vibration, and motor current, to detect ragging in pumps. Early detection of ragging would help the planning team to better utilise their technicians and lower costs associated with this reactive work. The risks associated with de-ragging pumps would also be reduced if the pumps can be de-ragged during the day instead of night. The WWPS can be up to 15 m below ground level, therefore working inside requires a confined space entry permit. This is due to the potential presence of flammable gases above the lower explosive limit (LEL), toxic gases (H2S) and deficiency of oxygen. Other risks include that of skin contact with wastewater while dismantling, assembling, and cleaning the pump, engulfment because of failure of an isolation

mechanism and falls from height. Activities during night-time are considered high-risk and pose additional risks due to low visibility and security issues.

2. Process

The first stage of this project was to select the pumps for analysis and organise for the vibration sensors to be installed. Motor current data is readily available from the PI-Excel software which communicates to SCADA to access the motor current data collected from WWPS. Vibration data required the placement of accelerometers specially for these tests. Once in place, the sensors transmitted data to the cloud for remote access. Python scripts, developed in Jupyter environment by the author, were used to compile a set of vibration measures in the time and frequency domains. Data frames with motor current, vibration, calendar and running time, and the number of cycles were assessed statistically, and the results visualised using Python.

2.1 Condition Monitoring using Vibration Analysis

"Wi-Care 200" vibration condition monitoring systems were installed at all selected dry-well WWPSs. Figure 2 (a) shows a typical installation of the vibration system at a WWPS in Perth with a complete schematic diagram outlining the process from collecting the raw vibration data from pumps to making a data frame in excel shown in Figure 2 (b). In Stage 1 two single-axis accelerometers are installed in axial and radial directions on both pumps of the WWPS (Hodkiewicz & Pan, 2003). Both accelerometers are powered by a 20 V DC cable from the data acquisition module (DAQ) module for live monitoring. The data is sampled at 4000 Hz and fed to Wi-care cloud server for remote access in Stage 2 using an integrated mobile network.

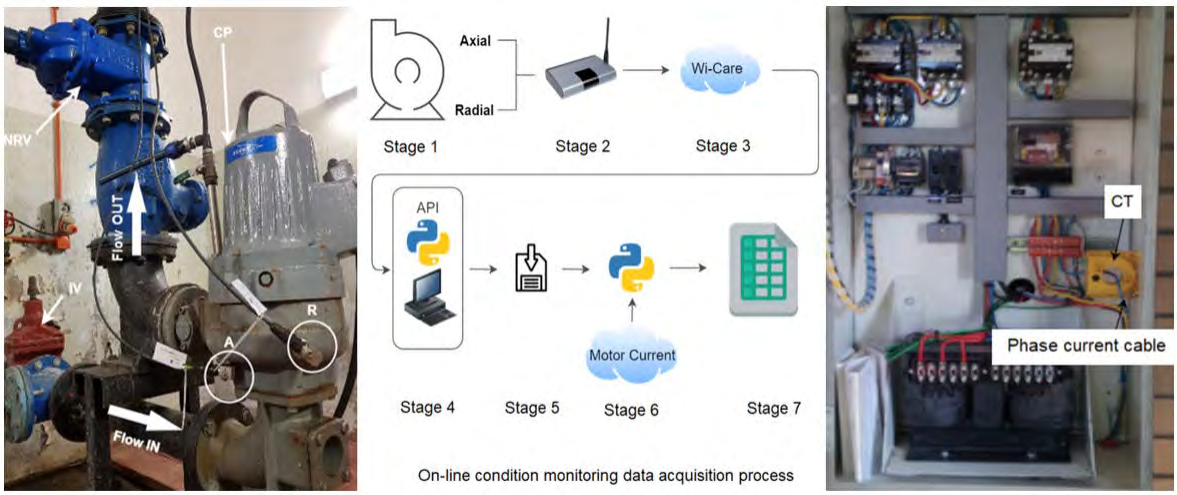

Figure 2 Accelerometers in Axial "A" and Radial "R" directions, Non-return Valve as "NRV", Isolation Valve as "IV" and Centrifugal Pump as "CP" shown in (a). Data management schematic diagram shown in (b) and installation of current transformers "CT" inside the control panel of pump stations to measure motor current shown in (c).

All WWPS vibration system installations were identical with regard to how the accelerometers were placed on the pump as shown in Figure 2 (a). The collected measurements stored on the cloud is in the JSON format in stage 3 which is converted into excel csv form by using the dedicated python script in Stage 4. The csv file is arranged and saved on the local computer in

such a way that one Excel file contains all the measurements taken from the pump in the axial and radial direction in Stage 5.

2.2 Condition Monitoring using Motor Current Data

A significant change in motor current can be observed between a pump in the "clean" state and completely ragged pump (Hedes, Svoboda, Vitan, Muntian & Anton, 2018). Motor current is measured by current transformers (CT) installed at the majority of the WWPS through SCADA network as shown in Figure 2 (c). The motor current data can be extracted using PI-Excel software available on WC server. Each WWPS are defined by specific tags on PI-Excel which relate to the various measurements being recorded on SCADA. A tag for motor current is used to extract the data in Stage 6. Lastly, the vibration and the motor current data are merged into a single data frame for processing in Stage 7.

3. Results and Discussion

Although 6 WWPSs were included in the experiment only three stations had both vibration and motor current data for the analysis (two stations didn't have motor current data and one station had technical difficulties in obtaining enough vibration data). The steady state motor current drawn by the pump when it is clean is usually close to its rated current however as pump starts to rag the steady state current goes up due to motor requiring an additional torque to maintain its rated speed. Figure 3 (left) shows Pump no. 1 (2.5 kW, single vane impeller) from station "A" draws 3.5 A current when the pump starts after cleaning and the current goes up to 6.1 A before the over-current protection prevents it from running to avoid the risk of fire due to overheating. The graph in Figure 3 (right) shows Pump no. 2 (4.5 kW, single vane impeller) from station "B" draws 5 A when it is clean and goes up to 14 A before failing due to ragging (station B has larger pumps thus over-current protection threshold is set at higher ampere value).

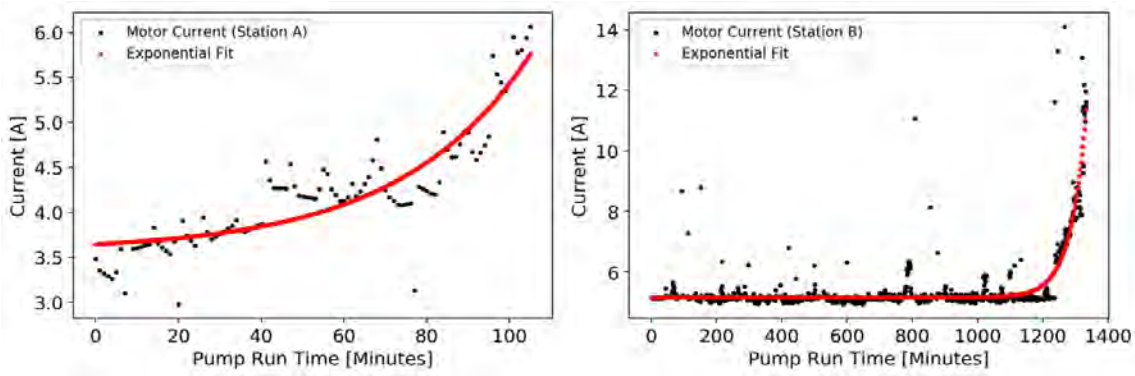

Figure 3 Motor Current trend shown by black dot of station A (left) and station B (right). An exponential fit made to data is shown in red line.

The horizontal axis on both graphs represents the 'total' pump run time in minutes from a clean to ragged condition. Our data suggests this 'total' run time of the pump varies considerably depending on several factors. Previous study within Water Corporation shows lack of awareness, societal attitude and inappropriate items entering the wastewater system are also the contributing factors which aggravates ragging (Marinko, 2018). Figure 4 (left) shows the exponential fits made to data representing the motor current trend of nine total failures of a same pump as a function of the pump's actual run time obtained from station A. Two features to notice are 1) an upward trend of motor current across, and 2) a wide variation in 'total' pump

run time for the same pump. Figure 4 (right) shows the trend of motor current of 5 ragging cycles from a different pump (4.5 kW) of station B.

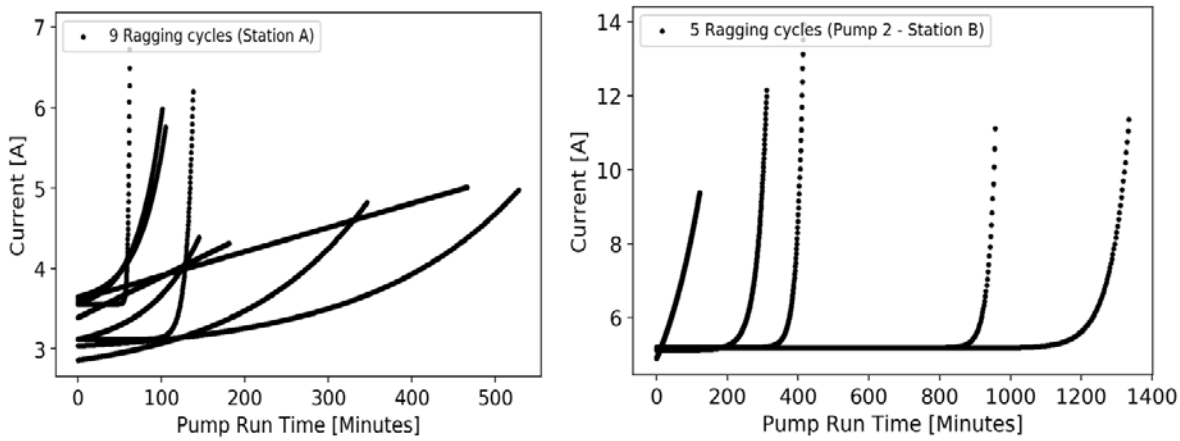

Figure 4 Superimposed 9 ragging cycles from pump 1 station A shown in graph on the left, 5 ragging cycles from pump 2 station B shown on the right

Vibration of the pump changes when the pump condition starts to deteriorate due to ragging. The vibration time waveform data collected from station A shows the difference in maximum amplitude of time waves of a clean and a ragged pump. Vibration response of the pump has been found to vary between pumps. Exponential fits made to vibration analysis variables such as RMS of time waves, running speed (1X) amplitude and running speed of the pump have been plotted as a function of total pump running time is shown figure 5. The change in vibration amplitude at running speed of the pump (24 Hz) of all 9 independent failure events is shown in (a), the Root Mean Square (RMS) of the time waves for all vibrations samples is shown in (b), and pump running speed approximated by a peak detection algorithm (FFT spectrum resolution is 1 Hz therefore the minimum change that can be detected is 60 RPM) can be seen decreasing towards the end of pump's life in (c).

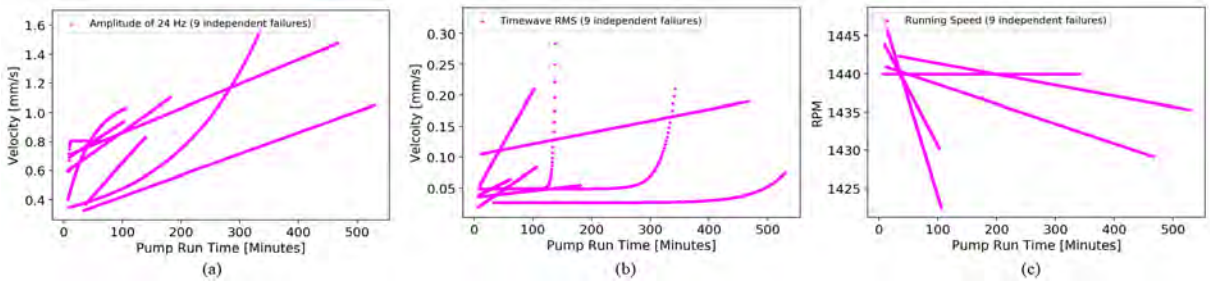

Figure 5 Trend (exponential fits) of 1X amplitude, RMS of time wave and RPM of pump from station A shown in (a), (b), and (c) respectively

The residual life of each ragging event of pump from station A is shown in figure 6 as a plot of Reliability R(t) against Run Time. An estimation of R(t) using motor current as an independent variable is shown in black, whereas the magenta triangle shows estimates of R(t) using both motor current and vibration parameters as independent variables. The blue line shows when pump ragged. The graphs show remarkably similar trends, notice the close similarity on trajectory for the motor current and vibration + motor current in the plot. This results are representation of 9 failure events from one pump and it suggests that the additional information obtained from vibration may not be worth the time and costs involved.

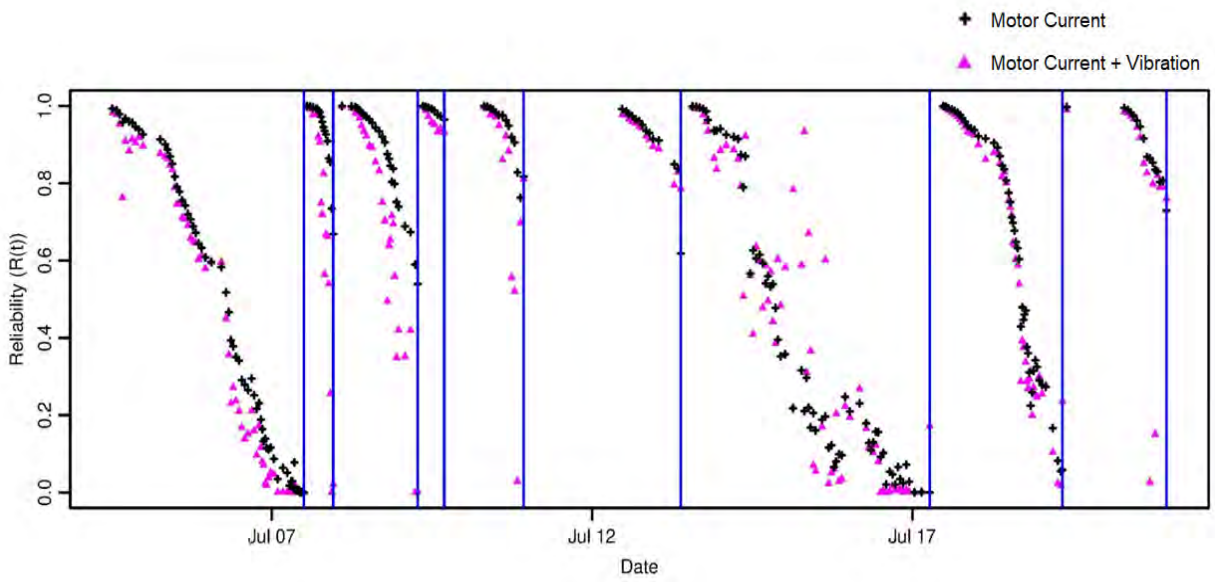

Figure 6 Residual life of pump (9 ragging events) of station A. Black represents reliability of pump using motor current as a covariate and, magenta represents motor current and vibration parameters obtained from timewave data as covariates

4. Conclusions and Future Work

Statistical analysis showed the parameters obtained using vibration data have lower statistical significance than that of motor current. A significant cost saving can be achieved by using SCADA motor current data at smaller pump stations to predict ragging. A long-term development could be building a website with real time monitoring dashboard which takes motor current data as its input and supported by Python scripts working in the backend to approximate when the next ragging event will occur.

5. Acknowledgements

This project would not have been made possible without the support from Professor Melinda Hodkiewicz, A/Professor Adriano Polpo, Dr. Teresa Martins Dias and ongoing mentoring from Principal engineer Mr Craig Hay and engineer Mr Benjamin Chan from Water Corporation. I would also like to thank Dr Jeremy Leggoe and Ms Amanda Bolt to provide me with an opportunity to work on this project and WC's OSH and M&E team for their support.

6. References

Hedes, A., Svoboda, M., Vitan, D., Muntian, S., & Anton, L. (2018). In situ Measurements on the Electrical Motors of Hydraulic Pumps Installed in a Wastewater Station - IEEE Conference Publication. Retrieved 7 August 2020, https://ieeexplore.ieee.org/document/8494589

Hodkiewicz, M., & Pan, J. (2003). Identification of transient axial vibration on double-suction pumps during partial flow operation. Retrieved 7 August 2020, from www.researchgate.net/publication/236009617 Identification of transient axial vibration-on double-suction pumps during partial flow operations

Marinko, E. (2018). Investigation of Root Causes of Wastewater Pump Station Obstruction and Ragging Faults. Retrieved 1 September 2020, from http://ceed.wa.edu.au/wp-content/uploads/2018/09/13.Marinko.WaterCorp.CausesWWPumpFaults.pdf

MIEX Resin Pump Assessment

Samuel Holden

Jeremy Leggoe
Chemical Engineering
The University of Western Australia

Brendan Vernall & Troy Jansen
CEED Client: Water Corporation

Abstract

Magnetic Ion Exchange (MIEX) technology is used at a Western Australian Groundwater Treatment Plant for removing dissolved organic carbon (DOC) particles (and other anions) from raw water via the use of magnetic resin beads. Although the resin in the plant is regenerated, MIEX resin must be regularly added in batches (to ensure optimal DOC removal) as it is continually 'lost' to the downstream section of the plant. This resin loss is believed to be due to attrition possibly caused by the current pumping arrangements. The objective of the project is to obtain results that inform whether new pumps should be considered to replace the existing pumps at the site. This is to be carried out by developing computational fluid dynamics (CFD) models to quantify shear fields of the pumps currently used, as well as the shear fields associated with alternative pump types or methods of fluid transport. Furthermore, microscopic analysis of the resin particles at different stages of the MIEX process is undertaken to understand particle properties, particle size distribution, and the ways in which the particles fracture.

1. Introduction

The Groundwater Treatment Plant (GWTP) uses two processes for treating incoming water – Magnetic Ion Exchange (MIEX) and advanced coagulation. It is the first large-scale MIEX facility in the world, processing up to ~100 ML/day of water in the MIEX circuit (Boarlage, 2003; Cadee et al., 2001). The plant uses a MIEX resin to remove dissolved organic carbon (DOC) particles, along with other water impurities, from a blend of bore water sources. The resin particles are magnetic, which enables these fine particles to agglomerate and settle at relatively high velocities for recovery and subsequent recycle in settler units (Boarlage, 2003; Quach, 2018; Quach 2019). Approximately 5-10% of the recovered resin is directed to the regeneration stage, with the remaining resin recycled to the contactor.

The structure of the MIEX DOC resin features a microporous methyl acrylate resin bead crosslinked with divinylbenzene (DVB). MIEX resin is highly selective for negatively charged DOC and has no affinity for other anions except sulphate. The DOC, together with some additional minor contaminants, is removed via exchange with chloride ions on active sites of the resin surface. The MIEX process is illustrated schematically in Figure 1.

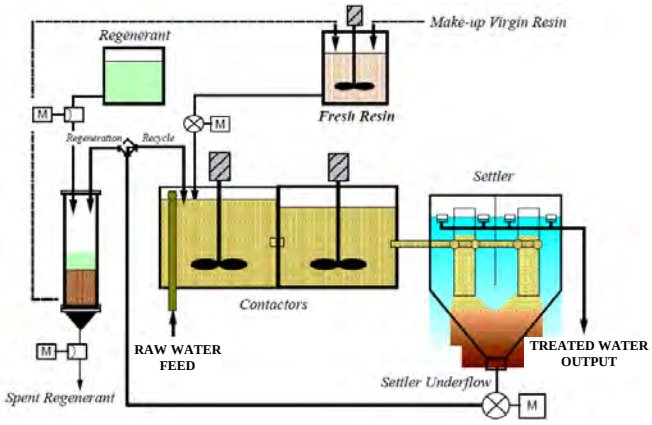

Figure 1 MIEX Flow Diagram (Slunjski et al., 2015)

Currently, the Water Corporation purchases 'top-up' resin to be added to the MIEX circuit as the resin is lost to the downstream section of the plant. As part of Water Corporation's continued commitment to process efficiency and improvement practices, the organisation has realised an opportunity to reduce operating costs following a more detailed understanding of the cause(s) of resin loss.

The issue of resin loss has been apparent at the GWTP since its inception. Prior studies on the MIEX resin at the plant have considered the design and operation of the settlers, as well as MIEX resin impurities caused by particle attrition (expected from pumps). While useful, these reports do not detail reasons for resin attrition, making this area ripe for research in an attempt to reduce annual resin costs. To positively identify the pumping system as the reason for resin attrition and to generally understand the ways in which the resin particles can erode, resin sample collection and subsequent laboratory analysis is required. Particle size distributions at various points in the MIEX circuit will be analysed to evaluate particle degradation and qualitatively indicate the means of particle break down.

It is believed that a potential source of resin attrition lies in the pumping system, due to the inherently high shear and turbulence associated with centrifugal pumps. In the MIEX system, there are three pump sets which contact resin particles: resin recycle/settler, fresh resin feed, and exhausted resin pumps. All three pump sets are centrifugal and fitted with 'low-shear' impellers. A summary of the pump operating conditions is presented in Table 1.

	Size (mm)	**Motor Rated Output (kW)**	**Speed (rpm)**	**Flow (m^3/h)**	**Head (m H_2O)**
Resin Recycle/Settler Pumps no. 1-6	150 x 100 – 245	3	980	100	9
Fresh Resin Feed Pumps no. 1, 2	80 x 50 – 200	3	1420	36	12
Exhausted Resin Pumps no. 1,2	80 x 50 – 200	3	1420	36	12

Table 1 MIEX Resin Transfer Pump Specifications

Due to the age of the existing resin recycle/settler pumps, no accompanying 3D drawings are available. Consequently, Keto Pumps was contracted to perform a 3D scan of the pump geometry to assist with the computational fluid dynamics modelling effort. A schematic of the existing resin recycle pump is depicted in Figure 2 (1).

Contact was made with various pump suppliers to explore the potential to use alternate (new) pump technologies, but detailed drawings or CAD files could not be obtained due to intellectual property limitations. (CAD files are necessary for CFD modelling as results are likely to be inaccurate if detailed internals of the pump geometries are not applied.) Keto Pumps has supplied CAD drawings for a range of different centrifugal pumps that meet the duty requirements of this application. These pump types include: K-TC4 (torq cyclo pump), K-HSF3 (open vane froth pump), and K-HS3 (closed vane slurry pump).

K-TC4 – Torq Cyclo Pump

The TC4 pump features a recessed vortex-style impeller which delivers 9.1 m of differential head at an impeller rotation speed of 700 rpm. Recessed impeller pumps typically exhibit low-efficiencies due to the lack of fluid contact with the impeller compared to their closed impeller counterparts. The TC4, operating at the specified conditions, is anticipated to have an overall efficiency of ~47%. This low impeller rotational speed, together with the recessed impeller design, is expected to minimise resin degradation and thus the TC4 may be an appropriate pump selection for practical implementation. A schematic of the TC4 pump is shown Figure 2 (2).

K-HSF3 – Open Vane Froth Pump

While the HSF3 pump was originally designed for minerals processing applications, it has been suggested as a possible alternative to the TC4 pump due to its open impeller configuration (non-recessed). The configuration is similar to the existing resin recycle pump but features a less angular impeller which may reduce resin erosion. The HSF3 pump has a higher rotational speed (980 rpm), improved efficiency (~54%), and is shown in Figure 2 (3).

K-HS3 – Closed Vane Slurry Pump

The HS3 pump has a typical closed impeller design. This pump was selected for CFD analysis as a confirmation that an open impeller design is superior for use in this resin transport application. It is unsurprising that, at an efficiency of ~68% for a 1020 rpm impeller speed, this style pump has the best head curve performance characteristics. A schematic of the closed vane slurry pump is presented in Figure 2 (4).

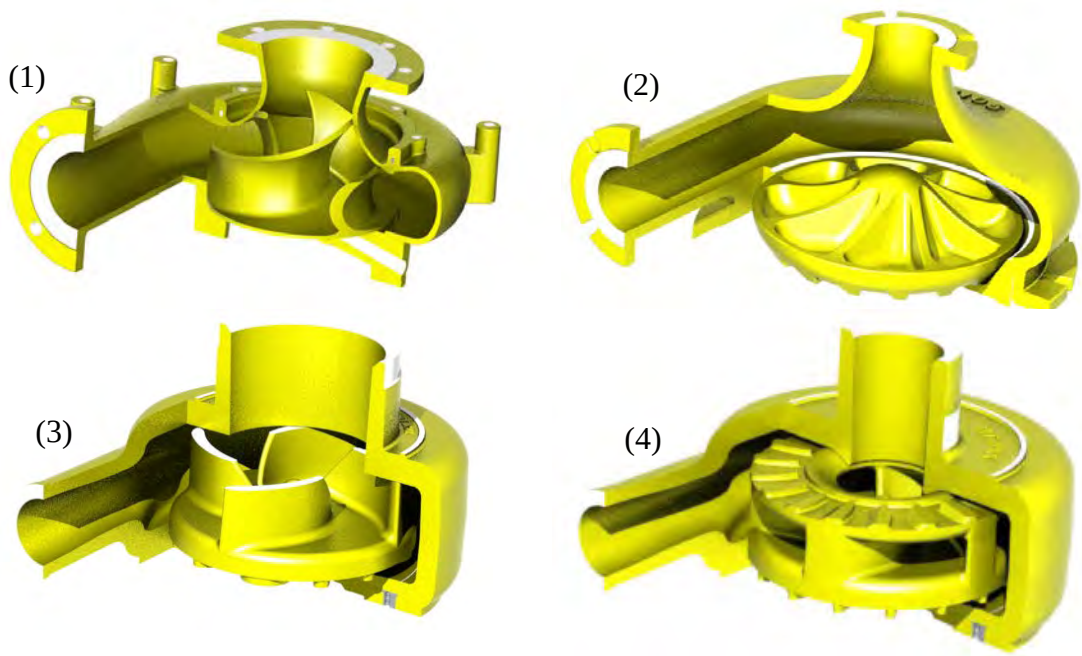

Figure 2 (1) Existing Resin Recycle Pump, (2) Torq Cyclo Pump, (3) Open Vane Froth Pump, (4) Closed Vane Slurry Pump

2. Laboratory Analysis

Characterisation of the MIEX resin particles is currently being carried out at the Centre for Microscopy, Characterisation, and Analysis (CMCA) at UWA. Scanning electron microscopy is used to determine properties, including particle composition, fracture patterns, and size distributions. Prior to conducting CFD simulations, resin analysis is important to evaluate the validity of the supplied particle size distribution, that the resin being 'lost' to the downstream sections of the plant is of expected size and magnetism, and that the primary reason for resin attrition is due to the currently installed pumping system.

MIEX resin is supplied to the GWTP as brown opaque beads in 1000L intermediate bulk containers (IBCs) which contain 90%$^{v}/_{v}$ resin in water. The resin contains 24-25% magnetic material with mean particle sizes specified to be in the range of 200-250 µm. In 2012, the resin supplier contracted CSIRO to determine a particle size distribution of virgin resin which indicated mean and median diameters of 211.5 µm and 191.2 µm respectively (CSIRO, 2012).

The plant locations that have been considered for resin sampling include: IBC, pre- and post-pump, and settler supernatant. IBC resin sampling indicates the extent of similarity between particle size distributions of the resin at the plant with that supplied by the vendor, and also provides insight into particle shape and composition before exposure to the MIEX process. The pre- and post-pump samples not only show qualitative particle degradation, but also indicate whether there is any reduction in particle size through the pump.

3. Computational Fluid Dynamics (CFD)

The Reynolds-Averaged Navier-Stokes (RANS) equations form the basis for all CFD modelling to describe the relationship between pressure and the instantaneous velocity field. Reports by Kim et. al (2014), Shah et al. (2010), and Ayad et al. (2015) favour use of the k-ω model with shear stress transport (SST) and second order discretisation solution methods. The idea behind this turbulence closure model is that it combines k-ω for describing flow near walls and k-ε for describing flow in a flow field / fully developed turbulent flows.

ANSYS Fluent®, as the industry standard software for CFD, has been selected for use in analysis of the flow field in this research. A summary of the Fluent® parameters used in the simulations are indicated in Table 2.

Parameter	**Chosen Option**	**Parameter**	**Chosen Option**
Turbulence Closure Model	SST k-ω	Simulation Time Scale	Transient
Discretisation	Second Order	Residuals	Local Scaling (10^{-5})
Inlet	Pressure Inlet	Timescale Factor	1
Outlet	Mass Flow Outlet	Timestep Size	0.0001
Casing	Non-Slip Boundary	Iterations per Timestep	10
Solution Scheme	Coupled	Number of Iterations	20000
Spatial Discretisation Gradient	Green-Gauss Node Based	Initialisation	Hybrid

Table 2 ANSYS Fluent® Setup Parameters

Mesh convergence is to be evaluated using Roache's Grid Convergence Index (GCI) which sees the number of elements in a coarse to medium to fine mesh approximately double through each stage. This is accomplished by reducing the element size by a factor of $\sqrt[3]{2}$. Therefore, it is anticipated that the resulting number of elements in each model will be ~600,000 for the coarse mesh, ~1.2 million for the medium mesh, and ~2.4 million for the fine mesh.

4. Results and Discussion

Laboratory analysis has been conducted on 2 sets of samples from the IBC, pre- and post-pump, and settler supernatant on dates 15/05/2020 and 21/07/2020. The samples have been taken from both the top (15/05/2020) and bottom (21/07/2020) of the IBC to observe any possible particle size differences. The virgin resin beads present in the IBC are spherically shaped which is to be anticipated as these particles have not yet entered the MIEX process and so no erosion has occurred. However, both samples of the virgin resin have indicated a similar particle size distribution that is noticeably smaller than expected (virgin resin size is in the range of 72-75 µm). Smaller particles are more prone to loss from the MIEX circuit which would lead to the increased addition of virgin resin and thus greater operating costs. Particle size distributions and microscopy images for the various samples are shown in Figure 3.

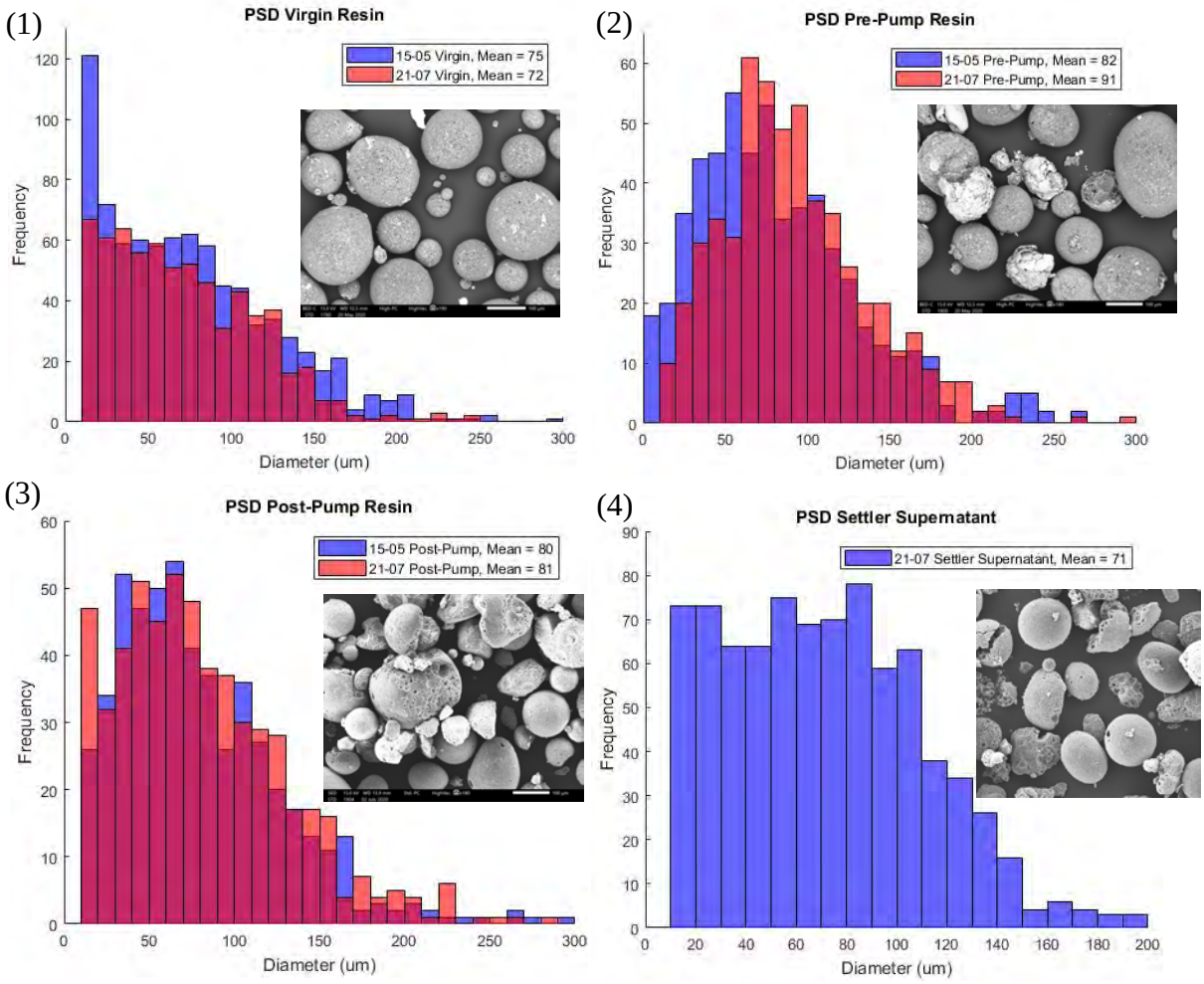

Figure 3 PSD and Microscopy of (1) Virgin Resin, (2) Pre-Pump Resin, (3) Post-Pump Resin, and (4) Settler Supernatant

Particle size analyses indicate a slight reduction in particle diameter through the pump which would imply that the pump is a prominent source of resin attrition. The settler supernatant has a larger than expected particle size as it is similar to that of the virgin resin. There is also a significant quantity of non-eroded resin particles which may suggest that some of the resin is not being used effectively in the process and is prematurely transporting to the settler supernatant.

4. Conclusions and Future Work

Laboratory particle analyses have yielded some surprising results which indicates reason for additional sample gathering (4-5 total samples) to confirm current findings. More rigorous sampling and PSD measuring techniques using purpose-built particle size analysis equipment (e.g. Horiba® instruments) is, therefore, required to confirm deviation from the expected particle size.

CFD models for the different pump types are producing head values slightly lower (~20%) than expected with convergence at 10^{-5} residuals. CFD modelling using smaller element sizes (finer mesh) is currently being undertaken to better align the pump head with the relevant manufacturers pump curves in an effort to produce reliable strain rate results for the different pump options.

5. Acknowledgements

I would like to express my appreciation to my academic supervisor Dr. Jeremy Leggoe, as well as Brendan Vernall and Troy Jansen from the Water Corporation, for providing the tools and guidance necessary to undertake this research. I would also like to extend thanks to Pete Kilner and the Keto Pumps team for their assistance and for providing proprietary information that will prove instrumental in the success of this project.

6. References

Ayad, A.F., Abdalla, H.M., El-Azm Aly, A.A. (2015). Effect of semi-open impeller side clearance on the centrifugal pump performance using CFD. *Journal of Aerospace Science and Technology*, **47** pp. 247-255.

Boarlage, S.F.E. (2003). MIEX Resin Loss Minimisation Study.

Cadee, K., O'Leary, B., Smith, P., Slunjski, M., Bourke, M. (2001), World's First Magnetic Ion Exchange (MIEX®) Water Treatment Plant to be Installed in Western Australia, Water Corporation of Western Australia, Orica Watercare.

CSIRO. (2012). Deer Park Particle Size Analysis.

Karassik, I.J., Messina, J.P., Cooper, P., Heald, C.C. (2008). Pump Handbook. McGraw-Hill Professional: US.

Kim, J.-H., Lee, H.-C., Kim, J.-H., Kim, S., Yoon, J.-Y., Choi, Y.-S. (2015). Design Techniques to Improve the Performance of a Centrifugal Pump Using CFD. *Journal of Mechanical Science and Technology*, **29** (1) pp. 215-225.

Quach, L. (2018), Resin Monitoring Analysis – MIEX DOC Resin Samples, Ixom Watercare.

Quach, L. (2019), Resin Monitoring Analysis – MIEX DOC Resin Samples, Ixom Watercare.

Shah, S., Jain, S., Lakhera, V. (2010). *Proceedings of International Conference on Fluid Mechanics and Fluid Power* [Conference Presentation]. Chennai, India.

Slunjski, M., Cadee, K., Tattersall, J. (2001), MIEX® Resin Water Treatment Process, Orica Watercare, Water Corporation of Western Australia, Black & Veatch

Behaviour of Ultrasonic Measurement in Composite Pipe

Liam Jason

Jeremy Leggoe
Chemical Engineering
The University of Western Australia

Des McEwan
CEED Client: Water Corporation

Abstract

Flow rate measurement provides important data for wastewater pump stations (WWPSs), as readings can be used for planning, quantification of overflows, and pump performance measurement. A variety of devices can be used for flow measurement at WWPSs. Water Corporation is investigating the possibility of using clamp-on ultrasonic flow meters (USMs), as they are more cost and labour effective compared to other devices. The accuracy of clamp-on USM measurements is affected by flow disturbances and the material characteristics of pipework. This study aims to further investigate the effects of material properties of common WWPS pipework on USM measurements. USM performance will be predicted by taking measurements on different pipe material that has been installed on an existing test rig simulating the actual pipework of a WWPS. Numerical models using Computational Fluid Dynamics (CFD) will assist in predicting the performance of USMs, as comparisons are made with physical testing. USM measurements recorded on polyvinyl chloride (PVC) indicated PVC does not affect the performance of the device. It is possible that pipe materials such as mild-steel (MS) and mild-steel cement-lining (MSCL) will lower the accuracy of USM measurement.

1. Introduction

Water Corporation utilises a variety of flow meters to monitor the performance of wastewater pump stations (WWPSs). Presently, magnetic flow meters (magflows) are the most widely used flow monitoring device at Water Corporation. They achieve a high level of accuracy and are directly installed in-line with pipework on the pressure main. Replacing magflows is a difficult task with only a small window available when the WWPS is offline. Installing flow meters directly in-line of the pressure main at WWPSs requires bypass which can cost approximately $35,000 to $70,000 depending on the size of the pump station. A cost-effective method of flow measurement is incorporating clamp-on (non-intrusive) ultrasonic flow meters (USMs), offering significant cost savings from easier installation and reducing risk of wastewater spillage by not disrupting the pipeline. The installation of clamp-on USMs could significantly reduce the costs associated with the need to bypass WWPS pressure mains for the maintenance of magflows.

Physical pipework and flow disturbances from pipe fittings can affect the accuracy of USM flow measurement. This presents challenges for clamp-on USMs as WWPSs have many fittings that create flow disturbances and the mild-steel cement-lined (MSCL) pipe can hinder transmission of ultrasonic waves. There are two types of flow rate measurement methods

utilised by USMs, including doppler and transit-time. For this research, the USMs being investigated utilise the transit-time method of flow rate measurement. This method internally calculates the flow rate through differences in time that the sound wave takes to travel between the two transducers. It is recommended that these USMs be used when the percentage of solid particles and/or gas bubbles are less than 10 wt% (Flexim, 2016). Manufacturers of USMs recommend locating these clamp-on devices at a certain length of straight pipe, upstream and downstream from pipe fittings. A fully developed flow profile is then achieved within the testing region of the USM, which is assists in achieving a suitable level of measurement accuracy (Flexim, 2016).

Yang (2019) tested a singular USM installed using two configurations and various downstream locations from a tee joint and at different orientation angles. The two USM configurations tested were the reflective and diagonal arrangement of transducers. The orientation angle of the meters refers to the position USMs were placed around the circumference of the pipe. A reference magflow was installed 60 diameters (60D) downstream from the tee joint to quantify the accuracy of the USM measurements. The error when the USM was placed in the reflective configuration, at a downstream length of 2D from the tee joint ranged between -1 to 18%. The lowest error values of -1% were recorded when the USM was placed at orientation angles of 0, 45, and 135°. The USM produced a significantly worse error when placed in the diagonal configuration at a majority of the orientation angles. As the flow meter was placed further downstream of the tee joint, the performance of the meter improved, with error values ranging between ±10% at 20D. Flow rates recorded at 20D were consistent at all orientation angles with the USM placed in the reflective configuration. It was concluded that the location of USMs at longer downstream distances from disturbances achieved more accurate flow measurements, but acceptable accuracy could be achieved at shorter distances (Yang, 2019).

Understanding the effects of pipe material is an important aspect of USM accuracy. USMs are installed on the exterior of the pipe, bringing several factors into play. The factors affecting USM performance include size, material, wall thickness, lining/coating, and surface roughness. For strong ultrasonic transmission through a pipe, the pipe material must be sonically conducting. Acoustic penetration is achieved when the pipe and fluid does not attenuate the sound before it reaches the following transducer. From Snell's law, when sound travels through various media, part of the energy is refracted, reflected, or absorbed. Materials such as concrete dampen sound energy, and occlusions in cast iron can attenuate the sound signal (Sanderson & Yeung, 2002). The introduction of linings/coatings must be airtight, as air pockets from delamination can further attenuate ultrasonic signals (Flexim, 2016). The pipe roughness impacts the degree of sound energy that is scattered, which is related to a ratio between the wavelength of the sound energy and the relative roughness of the pipe. Pipes with a high relative roughness will produce high scattering of sound ultrasonic signal. For significantly rough pipes, the profile factor must consider pipe wall roughness, as errors can reach 4%. Thus, in the presence of rough materials, such as cement, lowering the frequency will increase the wavelength, causing reduced sound signal attenuation; assuming sound velocity is constant through any given medium (Sanderson & Yeung, 2002).

2. Process – Test Rig Modifications & Experiments

An existing test-rig has been constructed to closely model a type 40 WWPS, with a scaling factor of 1:3 and a design flow of 20 L/s and DN 150 mm (Yang, 2019). The actual flow rate and diameter of the pipework on the test rig were 2.7 L/s and DN 50 mm, respectively. Potable water is the fluid medium that is passed through the test-rig and the pipe material is polyvinyl

chloride (PVC). A magflow is placed near the outlet of the test-rig and is used as a reference to verify the flow rate readings recorded by the USM. The performance of USMs is characterised by the percentage difference between the USM reading and the ideally located magflow.

Modifications are to be made to the test rig for the current project. An interchangeable section of pipe will be installed 1800 mm from the inlet of the test rig. This will allow for different pipe materials of roughly DN 100 mm to be input into the system, enabling USM measurements to be recorded on each material. The materials tested will include PVC, mild-steel (MS), and mild-steel cement-lined (MSCL), with the latter material being the most commonly installed in WWPSs. Each section of pipe material tested will be 3000 mm long, with USMs to be placed at a ratio of upstream to downstream length of 5:1 on the pipe section. Since the pipe size of the interchangeable section will be twice the original size of pipe used, the flow rate will be increased to achieve Water Corporations WWPS standard velocity of greater than 0.75 m/s. The flow rate will be changed to 10 L/s, meaning the fluid velocity through the DN 50 mm and 100 mm sections of the test-rig will be roughly 5.0 and 1.8 m/s, respectively.

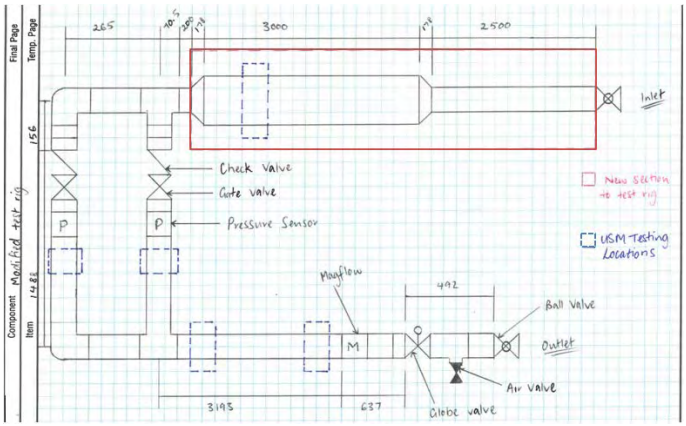

Figure 1 Schematic of test rig with modifications displayed as "New Section to test rig". USM testing locations have been specified in blue.

For the experiments, fully developed flow is desirable within the testing region of the USMs to ensure that any error in USM measurements should be mostly due to the pipe material. Thus, it is necessary that enough upstream length has been applied to achieve fully developed flow before the inlet of the interchangeable section and at the testing region of the USMs. The type of USM being tested utilises the transit-time method of flow rate measuring. A Computational Fluid Dynamic (CFD) simulation was constructed to verify that fully developed flow would occur at the test sections. Potable water and an air bleed valve will be used, making any effects from solid particles or air bubbles on the performance of USMs negligible.

The experiments will consider the performance of USMs when placed on different pipe material and the performance of two sets of USMs when placed in the same region at different orientation angles about the circumference of the pipe. All tests will utilise the reflective configuration as this offers the highest level of accuracy of the two USM configurations available. The experimental procedure is listed below:

- **Primary Testing:** USMs are installed on interchangeable pipe material following manufacturers' requirements. To isolate effects of pipe material, fully developed flow is established. Comparison of magflow and USM for verification of USM performance.
- **Secondary Test A:** Singular and dual sets of USM transducers will be placed on PVC pipe sections downstream of gate valve and tee joint, as well as interchangeable pipe section. Flow data will be collected from each configuration, averaged and compared

with magflow readings. For the dual CEED Seminar Proceedings 2020 Jason: Ultrasonic Measurement in Composite Pipe 4 set USM testing, the meters will be placed at the same downstream location on the test-rig, but situated 90° apart in orientation angle.

- **Secondary Test B:** USMs are installed over faults on MSCL pipe. Flow data is recorded and compared with data from non-faulty MSCL pipe. Faults are to be introduced at the testing region on the interchangeable pipe.

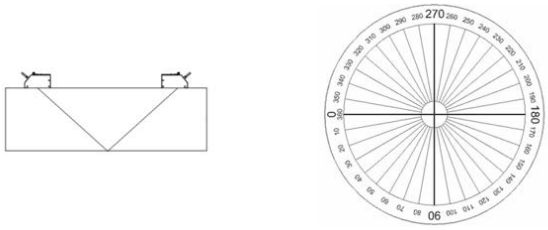

Figure 2 Representation of reflective USM transducer configuration on the left (Flexim, 2016). Reference of orientation angle looking at direction opposite to fluid flow.

3. Results and Discussion

Secondary test A has been completed, with single and dual set USM measurements recorded at multiple locations. The testing was conducted at the locations of 2D downstream from the tee joint (closest to the outlet), 7D downstream from the gate valve and 2D upstream of magflow. At 2D downstream of the tee joint testing location, there is a clear decrease in the range of error values with two USMs placed in the same testing location. The error values range from -1 to 12 % as opposed to just a single USM, which had a range of -1 to -18 % at the same location (Yang, 2019). The maximum error recorded from the dual set of USMs is roughly 6% less than the single set. Having two sets of USMs means that the flow measurement becomes less susceptible to flow profile disruptions as more sound paths are present, which is consistent with manufacturers' recommendations and literature, (Flexim, 2016) and (Baker & Thompson, 1975).

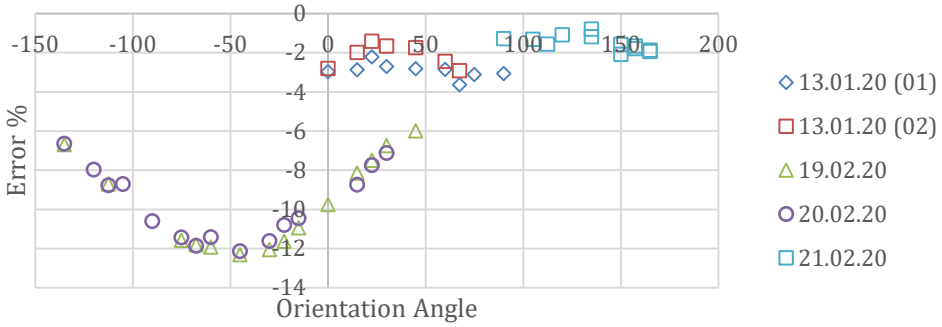

Figure 3 Error percentage values of dual USM testing at location 2D downstream of tee joint.

At 7D downstream of the gate valve, the variation in error percentage recorded was less than when compared to the 2D downstream from the tee joint case. The USMs placed at the 7D downstream from the gate valve case, the flow is given more length to re-establish, resulting in less volatility in error values measured. This is consistent with results found by Yang (2019), as measurements are less dependent on orientation angle as the distance from a flow disturbance increases. The error values taken from 7D downstream from the gate valve case with a dual set of USMs ranged from -6 to -8 %. At certain orientation angles, the error values obtained from

the 2D downstream of the tee joint case are less than the 7D downstream from the gate valve case.

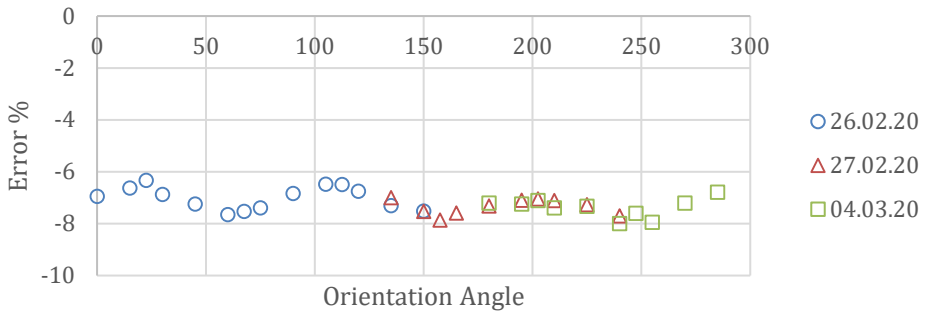

Figure 4 Error percentage values of dual USM testing at location 7D downstream of gate valve.

The error values recorded when the USMs were placed 2D upstream of the gate valve displayed similar behaviour to the results recorded from the 7D downstream of the gate valve. Again, there was less variation in error measurements obtained at all orientation angles, further solidifying the point that flow rate measurements become less dependent on orientation angle when placed further away from flow disturbances. The difference occurred in the error values obtained, as the USMs when placed 2D upstream of the magflow, the error values ranged between -4.8 to -6.0 %. The readings are slightly more accurate, but a difference is still present between measurements obtained from the USMs and the magflow, even when placed 100 mm apart.

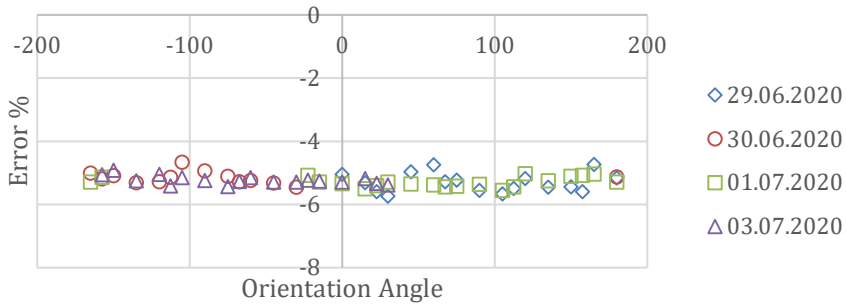

Figure 5 Error percentage values of dual USM testing at location 2D upstream of magflow.

4. Conclusions and Future Work

USM measurements are highly influenced by variation in the flow profile especially when placed close to a flow disturbance. Results depict that the accuracy of USM readings can improve when the meters are positioned further away from the flow disturbance. The results display that accuracy can be improved when the number of sound paths increases. USM measurements become less volatile when meters are positioned further away from the flow disturbance, with the dependence of orientation angle becoming negligible. The significance of the orientation angle is present when the meters are placed closer to flow disturbances for both single and dual set USM configurations.

Further interpretation of pipe material influence on USM measurement is required to offer further insight into USM behaviour when placed on composite pipe common to WWPSs such as MSCL. Construction of modifications to test rig shown above, will allow for multiple pipe

materials to be fitted and tested. It is known that PVC has little effect on USM measurement when compared to disturbances in the flow profile. This is displayed when USMs are placed at distances greater than 20D, as error values are consistently low when a fully developed flow profile is established. Reduction in accuracy of USM measurement could occur with tests on MSCL, as the ultrasonic wave must travel through two different mediums, with the cement-lining known to have high surface roughness and low acoustic conductivity.

Understanding the flow profile, especially when next to the flow disturbance, can assist in deciphering the best orientation angle that USMs must take. In terms of future direction, Potential for field trials at existing WWPSs would aid in understanding the performance of USMs, especially when testing in non-ideal conditions, such as aged pipe and reduced water quality. Along with field tests, investigation of the flow field within the test rig using CFD would assist in verification of the USM performance.

5. Acknowledgements

I would like to express my gratitude towards Des McEwan and David Muller for their advice on technical issues. I would like to thank Brian Tan and Barak Carder for their assistance towards the construction of modifications made to the test rig. Additional thanks to everyone from the In-service, Assets Planning branch, Shenton Park Water Research and Innovation Precinct and the Shenton Park Meter Lab who have expressed their willingness to help.

6. References

Baker, R. C., & Thompson, E. J. (1975). *A two beam ultrasonic phase-shift flowmeter.* Glasgow: National Engineering Laboratory.

Flexim. (2016). *User Manual UMFLUXUS_F6V4-5-1EN-Ultrasonic Flow meter for Liquids.* Flexim.

Group, A. D. (2017). *Pipeline Selection Guidelines.* Perth: Water Corporation.

Ruppel, C., & Peters, F. (2004). *Effects of Upstream Installations on the Reading of an Ultrasonic Flowmeter.* Flow Measurement and Instrumentation .

Sanderson, M. L., & Yeung, H. (2002). *Guidelines for the Use of Ultrasonic Non-Invasive Metering Techniques, Flow Measurement and Instrumentation.* Bedford: Department of Process and Systems Engineering, Cranfield University.

Stoker, D. M. (2011). *Ultrasonic Flow Measurement for Pipe Installations with Non-Ideal Conditions.* Utah: Utah State University.

Yang, T. (2019). *Use of Flow Measurement Devices in Restricted Environments.* Perth: Water Corporation.

Maximum Permissible Pipe Loadings

Kieron Ho

Mohamed Elchalakani
Civil, Environmental and Mining Engineering
University of Western Australia

Perry Beor
CEED Client: Water Corporation

Abstract

Adequate pipe cover is important for buried pipes to provide protection from surface loads. During construction and earthworks by others around Water Corporation pipe assets, the cover of these pipes may be affected such that relaxations in requirements or engineering solutions are proposed. For any such measures to be approved, knowledge of the contributing risk factors is fundamental. Establishing the barrel strength of pipes made from cast iron, cement lined mild steel and PVC of differing nominal diameters and estimating the buried cover depth necessary to protect them will provide a contribution to the knowledge base used in this decision making. With cast iron pipes of sizes DN 100 and DN 150 tested in a laboratory, it has been found that such pipes can quite adequately withstand expected vehicle loading conditions, but as with all engineering applications these results must be considered alongside a broad range of contributing factors.

1. Introduction

The Water Corporation protects its buried pipe assets from imposed surface loads primarily by ensuring they have sufficient cover between the surface and the pipe buried below. A pipe is provided adequate protection at installation through either sufficient cover or via an engineering solution. This might take the form of a trench, tunnel, bridging slab, sleeve or concrete encasing to strengthen the pipe (Water Corporation, 2018). Issues arise where earthworks may disrupt or remove the effectiveness of some of these measures. During such scenarios, the buried depth cover of a pipe may be reduced, introducing the risk of the pipe asset becoming damaged. The Water Corporation is seeking to increase overall knowledge of the cover requirements for their pipe assets to provide additional information when pipe cover requirements are being considered.

A relaxation regarding the cover requirements may allow construction works to continue, but any decision regarding relaxations or engineering solutions must be made with the knowledge of likely outcomes. Factors which affect any proposed relaxation of cover requirements include the expected magnitude of surface loads within the vicinity of the pipe, the material of the pipe and the size of the pipe. Of great interest to the Water Corporation are the properties of “legacy” pipes including cast iron (CI) and cement lined mild steel (MSCL), as well as the more modern polyvinyl chloride (PVC) pipes.

1.1 Current Water Corporation Practices

The cover requirements for pipe assets as currently required may be found in Water Corporation Design Standards, including DS 60, DS 63, DS 66 and DS 51, providing guidance for non-reticulation pipelines, reticulation pipelines smaller than DN250, urban drainage pipes and wastewater pump stations and pressure mains respectively. Further guidance on pipe bedding, laying, fill and appurtenances is located in the Water Supply Code of Australia (Water Services Association of Australia, 2011).

The development of these cover values is drawn from a design approach that also incorporates accessibility of appurtenances, allowances for erosion effects, risk based considerations for hazardous material transport, and other influences from lessons learned through experience. They are of conservative nature, to ensure a consistent construction standard for all installed pipes, which will allow for predictable location and behaviour for future activities.

1.2 Pipe Testing Scope

To fulfill the Water Corporation's wishes to test legacy pipes, the samples have been sourced from recent removal of such pipes from service. Apart from the benefit of replicating any effect that aging or fatigue may have on the properties of collected pipe samples, it is entirely possible that they are no longer available in new condition. While pipes made from polyvinyl chloride (PVC), polyethylene (PE) and steel (including MSCL) are currently being installed, asbestos cement (AC), reinforced concrete (RC) and cast iron (CI) are no longer being installed. Sample collection thus relies on the collection of recently removed pipe assets for older pipe materials.

The scope of this investigation will be limited to failure of the pipe barrel section under bearing stress. As used in Technical Basis of Austroads Guide to Pavement Technology (Jameson, 2013), a surface load replicating what is called "full standard axle loading" for trucks will be adopted as the imposed surface load. This axle configuration is a dual-tyred single axle carrying a total load of 80kN, defined by individual wheels producing a surface stress profile of circular radius 92.1mm and vertical contact stress of 750kPa (Jameson, 2013).

2. Process

To investigate cover requirements and the effect that modifying cover depth has on load transferal to a buried pipe, soil and buried pipe loading theories are utilised to link laboratory experiments to expected buried behaviour in the field. Made available for the purpose of this task is the Baldwin static loading machine for compression tests, meaning that the experiment phase of this research will not involve the effects of burying a pipe, and is adapted to reflect the condition of pipes found in service.

2.1 Truncated Cone/Pyramid Soil Theory

Also known as the Approximate Method (Budhu, 2015), the truncated cone/pyramid theory will provide a representation for sandy soil behaviour in minimum-cover analysis. It simplifies a surface load to a circular or rectangular shape, producing a truncated cone or truncated pyramid soil structure respectively in showing how the surface load is distributed through the soil. For minimum cover analysis, self-weight of the soil is negligible compared to the load required for pipe failure (Moser & Folkman, 2008). By using the standard axle loading defined

in (Jameson, 2013), a benchmark for surface loading is used in the development of the cover requirements. This truncated cone will develop vertically downwards with the cone radius increasing 1 for every 2 descended (Moser & Folkman, 2008). The purpose of this theory is to find a depth that the pipe is able to withstand as the soil cone structure dissipates vertical stress. This soil structure requires a development depth approximately equal to the width of the surface load (Budhu, 2015), and so the shallow limit on the cover depth can be set at 200mm.

2.2 Two-Edge Bearing Test

The test using the Baldwin static loading machine is adapted from a method used to determine the bearing strength of concrete pipes. This is found in AS4058 Appendix C (Standards Australia, 2007), and involves loading pads on the crown invert of the pipe. While in concrete the failure point is when significant cracks occur, the different pipe materials in this project will require differing indicators for critical failure. For example, if the pipe has a brittle failure (such as CI), the complete failure will provide an obvious end of loading, while the failure point of MSCL could be the destruction of the internal cement lining, and PVC the decreased flow capacity. The data collected during these lab experiments include the imposed load and the change in vertical height of the pipe, as well as any other observations during the course of the loading.

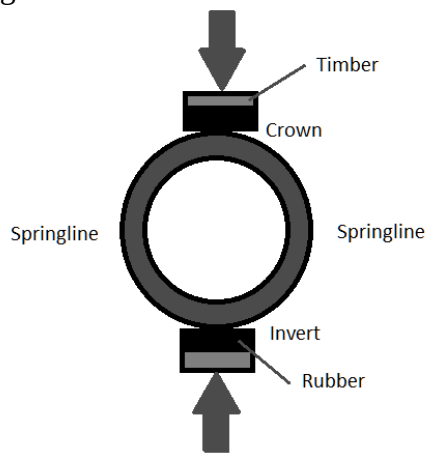

Figure 1 (a) Diagram of two-edge bearing method as found in AS4058 (Standards Australia, 2007)

Figure 1 (b) Set-up of the two-edge bearing method at the UWA structural lab

2.3 Bedding and Impact Factors

A buried pipe will not have a force concentrated on solely on the crown and invert, but will experience a distributed load on the top surface, with the surrounding soil supporting and strengthening the pipe against bearing failure along the bottom. To account for this, a modifying factor is adapted from a buried concrete pipe scenario using the live load bedding factor of 1.5 (Concrete Pipe Association of Australasia, 2013) due to the similar rigid properties of the pipes being tested, and with vehicle loads being live loads.

An impact factor must also be applied to account for the dynamic loading nature of vehicle tyre loads across buried pipes. For a shallow application, this is taken as a 1.5 multiplier on the imposed load (Moser & Folkman, 2008).

2.4 Combining the Theories

A representation of these theories based on AS3725 Cl. 10.2(a) (Standards Australia, 2007):

$$\{T_c F_B\}_{pipe\ strength} \geq \left\{ P \times \frac{\pi R^2}{\pi\left(R + \frac{z}{2}\right)^2} F_I B \right\}_{transferred\ load}$$

Where $T_c = experimental\ pipe\ strength\ (kN/m)$
$F_B = live\ load\ bedding\ factor = 1.5$
$P = vertical\ spressure\ of\ tyre\ on\ surface\ (kPa)$
$R = surface\ contact\ radius\ of\ tyre\ (m)$
$z = vertical\ distance\ between\ surface\ and\ top\ of\ pipe\ (m)$
$F_I = impact\ factor = 1.5$
$B = pipe\ width\ (m)$

3. Results and Discussion

At this point, only CI samples of sizes DN100 and DN150 have been tested. They produce a strength failure point brittle in nature, roughly longitudinal, following crown, invert and springlines. Experiments were conducted on samples of length 250mm and the results for both CI sizes are shown below.

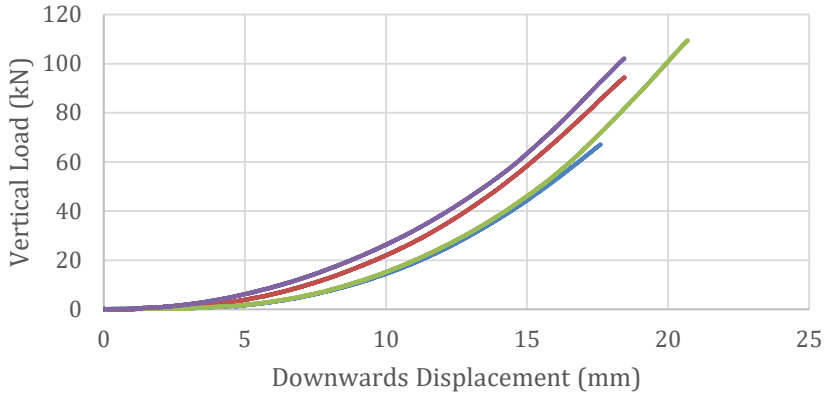

Figure 2 Load vs Displacement graph for CI DN100 Baldwin bearing tests

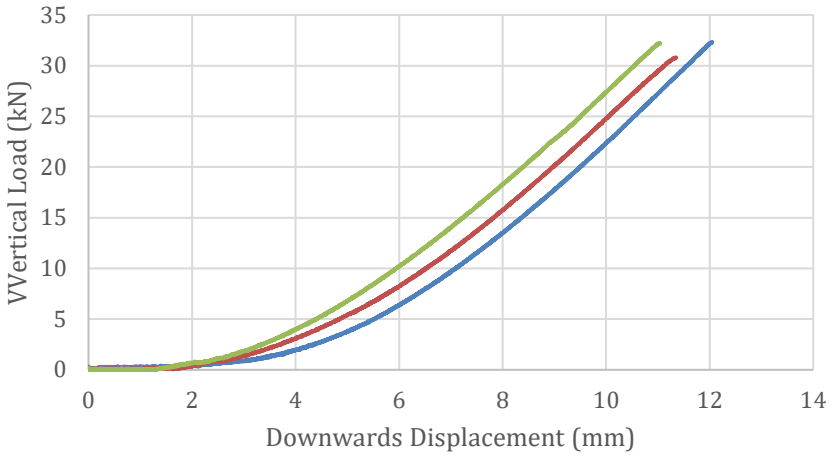

Figure 3 Load vs Displacement graph for CI DN150 Baldwin bearing tests

Pipe Specifications	Minimum Ultimate Strength	Minimum Ultimate Strength/m
DN 100 CI	67.1 kN	268.3 kN/m
DN 150 CI	30.8 kN	123.2 kN/m

Table 1 Converts the experiment ultimate strength load to a per-meter property

By using the standard axle load defined by a circle of 92.1mm radius and 750kPa pressure (Jameson, 2013), the equation becomes:

$$T_c \geq 750 \times \frac{0.0921^2}{\left(0.0921 + \frac{z}{2}\right)^2} B$$

Pipe Type	Bearing Strength/m	Z (m)	Transferred Load/m
DN 100 CI	268.3 kN/m	0	75 kN/m
DN 150 CI	123.2 kN/m	0	112.5 kN/m

Table 2 Compares the bearing strength of the pipe to the transferred standard axle load it would be resisting

3.1 Analysis and Recommendations

Based on the calculated strengths and transferred loads, both CI DN100 and DN150 are capable of carrying the standard axle load without requiring any additional burial depth. This does not however suggest that pipes placed on the surface will withstand the loading alone, instead that if the tyre pressure is distributed properly on the pipe then it will withstand the load. Thus, the minimum cover will be set by the depth required for the development of the truncated soil structure (Budhu, 2015) of 200mm. Buried at 200mm, the pipes will have the conditions:

Pipe type	Bearing Strength/m	Transferred Load/m	Factor of Safety
DN 100 CI	268.3 kN/m	17.2 kN/m	15.56
DN 150 CI	123.2 kN/m	25.9 kN/m	4.76

Table 3 Compares the strength of the pipe to a 200mm cover transferred load

The 200mm recommended pipe cover provides a high factor of safety, especially for the DN 100 CI pipe, but due to the brittle properties of the CI pipes it is important that unnecessary risks be avoided. Too shallow a cover may cause rocks to produce stress concentrations, and ruts may reduce the true cover with sufficiently loose soil and traversal (Moser & Folkman, 2008), so care must still be taken when working around these pipe types.

4. Conclusions and Future Work

For the pipes tested to date, a minimum cover recommendation of 200mm for each CI pipes of DN 100 and DN 150 may appear overly conservative, with factors of safety 15.5 and 4.7 respectively. However, the testing to date has been conducted on a small sample size of 4 x DN 100 and 3 × DN 150, so some work must still be done to develop a full picture of the representative strength of these particular pipes. If additional samples can be obtained within the project timespan there will be benefits not just to provide additional strength values, but to provide a more accurate observation of how age and wear affect the pipes that were in service.

It should be noted that any samples capable of being tested produce knowledge bias towards higher pipe strength results, since any pipes too deteriorated or damaged to be tested will not become tested samples and will therefore not appear in any results. Such a study on the full condition of in-service or recently in-service pipe assets would provide knowledge of great significance, however that is outside the scope of this project.

For the remainder of this study, a focus will shift to MSCL and PVC pipes, with the intent to observe and measure their behaviours under loading and how this compares to pipes of differing sizes and materials. Additional loading scenarios may also be considered, with heavy rollers, cranes or other heavy vehicles of interest.

Recommendations for future studies to complement the information covered in this project include additional pipe materials and sizes, fatigue loading effects, vibration effects, alternative failure modes such as socket failure or pipe beam failure, testing with a pressurised pipe barrel, more accurate laboratory replications of buried pipe loading conditions, and investigating the effect that soil properties have on loading assumptions.

5. Acknowledgements

I would like to recognise the many people who have given me assistance or knowledge despite hinderances and complications due to prevailing circumstances. These include, Glen Williams for providing an insight into operating pipe statistics, Tim Ryan for organising pipe samples and delivery, Simon Kenworthy-Groen from Main Roads for providing vehicle data, Andrew Lloyd from All Rubber for the experiment bearing pads construction, Stephen Naulls from the UWA structures lab for adapting my procedure to the equipment, Sandra Henville, Emer McClintock and John Walter for putting work into preparations for asbestos testing that sadly could not proceed, and those at Water Corporation not mentioned who have helped me out.

6. References

Budhu, M. (2015). *Soil Mechanics Fundamentals. 1st edition.* John Wiley & Sons, Ltd.

Concrete Pipe Association of Australasia. (2013, February). *Influence of bedding support on pipe class.* Retrieved from Technical notes: https://www.cpaa.asn.au/images/publications/technical_notes/TN_Influence_bedding_support_Feb13.pdf

Jameson, G. (2013). *Technical Basis of Austroads Guide to Pavement Technology Part 2: Pavement Structural Design.* Victoria: ARRB Group Ltd.

Moser, A. P., & Folkman, S. (2008). *Buried Pipe Design, Third Edition.* The McGraw-Hill Companies.

Standards Australia. (2007). *AS/NZS 3725:2007 Design for installation of buried concrete pipes.* Standards Australia, Standards New Zealand.

Standards Australia. (2007). *AS/NZS 4058:2007 Precast concrete pipes (pressure and non-pressure).*

Water Corporation. (2018). *Design Standard 63: Water Reticulation Standard Design and Construction Requirements for Water Reticulation Systems up to DN250.*

Water Services Association of Australia. (2011). Water Supply Code of Australia. *WSA 03-2011 Third Edition Version 3.1*. Sydney, NSW, Australia: Water Services Association of Australia Limited.

Heat Reduction Treatments for Electrical Cabinets

Rowan Sobey

Yuxia Hu
Civil, Environmental and Mining Engineering
The University of Western Australia

Chao Sun
Planning and Transport Research Centre (PATREC)
The University of Western Australia

Stefan Hoffman
CEED Client: Main Roads Western Australia

Abstract

Main Roads WA has many electrical cabinets and enclosures in the field across the state that are exposed to intense heat and high temperatures. This project investigates and models different solutions to reduce the heat loads on the cabinets and electronics housed inside. A trial with empty cabinets was setup to test experimental heat reduction treatments and data was collected on active traffic signal cabinets in the field to gain a basis for analysis. Models of the heat transfer between the cabinets and the environment were constructed using first principles and accepted methods to predict equilibrium temperatures. By combining real world trials and applying modelling to a variety of locations where cabinets are installed, an informed recommendation can be made on requirement and efficacy of solutions such as sunshades or heat reflecting paint.

1. Introduction

Main Roads Western Australia is investigating various options to reduce high temperatures in electrical cabinets. Excessively high temperatures in desert and remote areas adversely affect the operations of electronics, with potential drawbacks of loss of operational capabilities through shutdowns, expensive unscheduled maintenance and call outs, and possible degradation of operational lifespan. Main Roads' current approach of using high temperature equipment and monitoring is common in industry, however due to the range of different areas in which they operate more suitable solutions for high heat loads may exist.

Current academic literature around reducing or rejecting heat generally follows two areas: active solutions for heat dissipation in electronics, and passive solutions applicable to building and large structures. Examples of active solutions are airtight heat exchangers (Kobayashi & al., 2001) and phase change materials (Zhao, & al., 2016), while an example for large structure systems is underground air pumping and heat sinking (Hong, & al., 2008).

Neither of these dominant areas are applicable to a 1.3 m tall outdoor electrical cabinet; active solutions can compromise the IP ratings, or are power inefficient, and introduce another system to monitor. Most large structure passive solutions aren't applicable to cabinets due to relatively small budgets and tiny thermal mass. Industry solutions such as metal sunshades spaced away from the cabinet do exist (Delvalle, 2019), however academic research is limited.

2. Process

2.1 Experimental treatment trial

The experimental trial consisted of taking 4 decommissioned cabinets that had their electronic components removed and applying experimental heat reduction treatments. One cabinet was painted with Solacoat (heat reflecting paint); a second was clad with Rockwool insulation; a third had galvanized steel panels spaced 40 mm away and bolted to the cabinet as sunshades; and the fourth was left unchanged as a control cabinet.

The cabinets were placed near each other at Main Roads' Jandakot depot. Inside each cabinet a temperature data logger was installed on the centre of a tray two thirds the height of the cabinet. The loggers recorded their temperature every 30 minutes with an uncertainty of ±1 °C.

Due to the ad hoc nature of the trial, some aspects could be improved to better reflect high temperature cabinets in the field. The cabinets had no internal heat generation, they were free standing rather than bolted onto a plinth which fed cables into the ground, the cabinets were closely spaced and interfered with radiative heat to an extent, and there were buildings near by which would unpredictably change the wind and radiation environment.

2.2 Active cabinet data collection

Cabinets in the field that housed operational hardware for traffic signal intersections had high accuracy (±0.2 °C) data loggers installed, logging every 30 minutes. Similarly to the trial, the loggers were installed on a tray and avoided contacting hot surfaces and heat sources. A total of 9 cabinets in batches of 3 have been monitored to date.

In addition to monitoring a single temperature inside active cabinets, a cabinet with a vertical "top hat" extension had three temperature loggers installed concurrently at different heights to measure vertical variations in heat inside a cabinet. One was installed in the extension, another on the tray as before (now at half the height) and the third just above the floor. The method was repeated on a regular cabinet without the extension.

A contact temperature probe (±1 °C) was used to measure the outer surface temperature of the cabinets on each panel and several points inside. The time of day was kept between 1:30-3:00 PM to keep near the maximum cabinet temperature period. 9 measurements on the exterior of the cabinets and then 3 measurements inside the cabinet were taken at each sampling.

2.3 Heat and temperature modelling

2.3.1 Approach

The heat transfer and temperature modelling of the cabinets assumes that the cabinet is at its daily maximum temperature; this maximum was at or close an equilibrium; and no rapidly changing heat transfer was occurring. Following these assumptions, a steady state heat energy equation can be constructed where the incoming heat can be balanced to the outgoing heat by finding the cabinet temperature where the net heat transfer balanced. Each component of the equation is then considered individually. The overall equation and components can be written as Eq. 1. This approach is based on advice and a paper from Prof H.T. Chua (Chua, 2019).

$$\dot{Q} = 0 = Q_{solar} + Q_{internal} - Q_{rad} - Q_{ground} - Q_{conv} \quad (1)$$

The modelling was constructed in Excel and validated using the active cabinet data. The model assumes an average temperature across the entire cabinet and ignores variations across panels and internal temperature. Simplifications were also applied to the environment.

2.3.2 Heat transfer equation components

$$Q_{solar} = \alpha_{surface} \cdot (A_{beam}E_{beam} + A_{diff}E_{diff}) \cdot C_{cloud} \quad (2)$$

Q_{solar} – Represents solar irradiation, both beam and diffuse. The beam and diffuse components have relevant areas and emissive powers with a cloud cover factor applied if necessary. Data is retrieved from the Bureau of Meteorology (BOM).

$Q_{internal}$ – Represents heat generated by internal components by electric power consumption.

$$Q_{rad} = \frac{\sigma\varepsilon_{\mathrm{surface}}\mathrm{A_{sky}}(\mathrm{T_{cab}^4} - \mathrm{T_{sky}^4})(1-\mathrm{F_{w,ground}})}{(1-\varepsilon_{\mathrm{surface}})(1-\mathrm{F_{w,ground}})+\varepsilon_{\mathrm{surface}}} \quad (3)$$

Q_{rad} – Represents radiation emitted to the sky from the cabinet. It considers the local sky view factor and sky temperature. Sky temperature is determined from the dew point and cloud cover.

$$Q_{ground} = \alpha \cdot F_{w,ground} \cdot Albedo_{ground} \cdot (E_{beam} + E_{diff}) \quad (4)$$

Q_{ground} – Represents the diffusely reflected solar energy coming from the ground surrounding the cabinet. Although not necessary for the required level of accuracy, the albedo and view factor can be adjusted for each panel of the cabinet. Radiation exchange between the cabinet and ground is not considered since their similar temperatures would have negligible heat flow.

$$Q_{conv} = hA(T_1 - T_2) \quad (5)$$

Q_{conv} – Represents heat dissipated from the cabinet to the atmosphere through convection. It is determined by using semi-empirical methods from academic literature to calculate a Nusselt number for each panel, giving an accurate heat transfer coefficient, *h*. Forced, natural and mixed convection are use ground wind speed.

3. Results and Discussion

3.1 Experimental treatment trial

The experimental trial showed that a consistent trend between the different treatments. The control cabinet consistently had the highest temperature as expected, followed by the insulation cladding, heat reflecting paint, and (the lowest temperature): the sheet metal sunshades. The temperatures are plotted below in Figure 1 and tabulated in summary in Table 1.

While the drawbacks with the setup outlined in the Process couldn't be mitigated in the circumstances, the trial provided useful practical information early in the study to guide further investigation and decisions. This trial demonstrated that the sheet metal sunshade was effective at eliminating almost all the incoming radiant heat from the sky and ground, while the paint and insulation split the difference between the sunshade and control cabinets. The insulation's weather resistance was poor, so further consideration was discontinued as long-term durability is a key consideration for Main Roads.

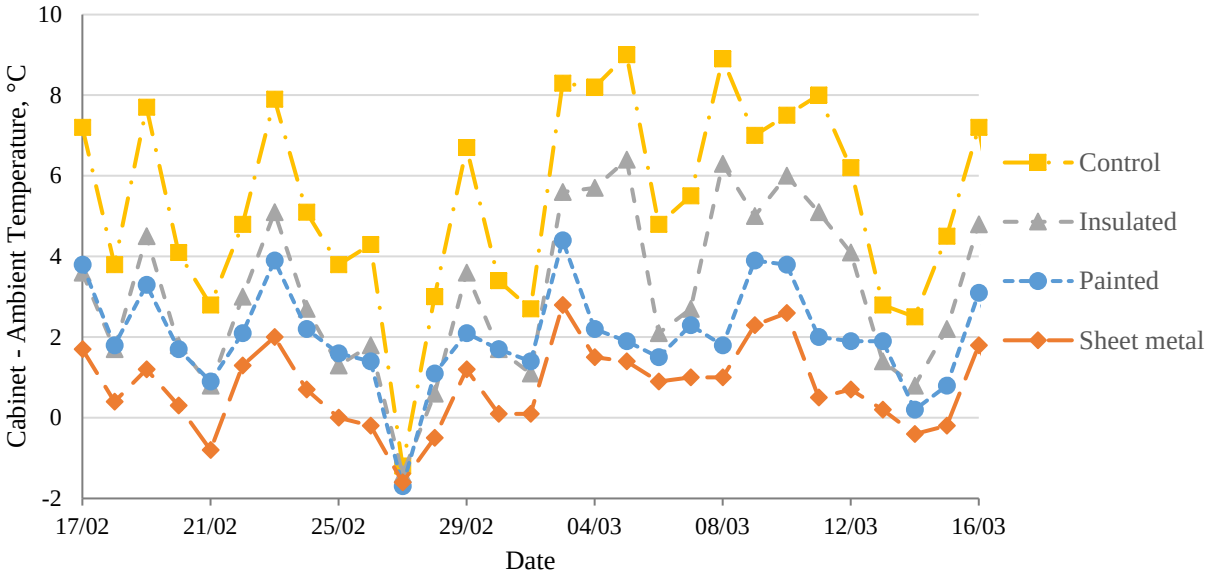

Figure 1 A plot of daily maximum temperature of the 3 experimental trials and a control. Temperatures are shown relative to ambient air temperature.

Date	Ambient	vs. Ambient			
		Control	Insulation	Paint	Sheet
17/02 - 09/04	30.08	+5.32	+3.15	+1.94	+0.78

Table 1 A table summarising Figure 1 using averages over the date range.

3.2 Active cabinet data collection

The temperature data loggers installed in active cabinets gave several insights into not just the heat from the environment, but also heat distributions inside the cabinet. Figure 2 shows the daily cabinet and ambient maximum temperatures. It is immediately noticeable that the temperature differences between the cabinets and ambient air is much greater than the trial due to internal heat generation in the active cabinets.

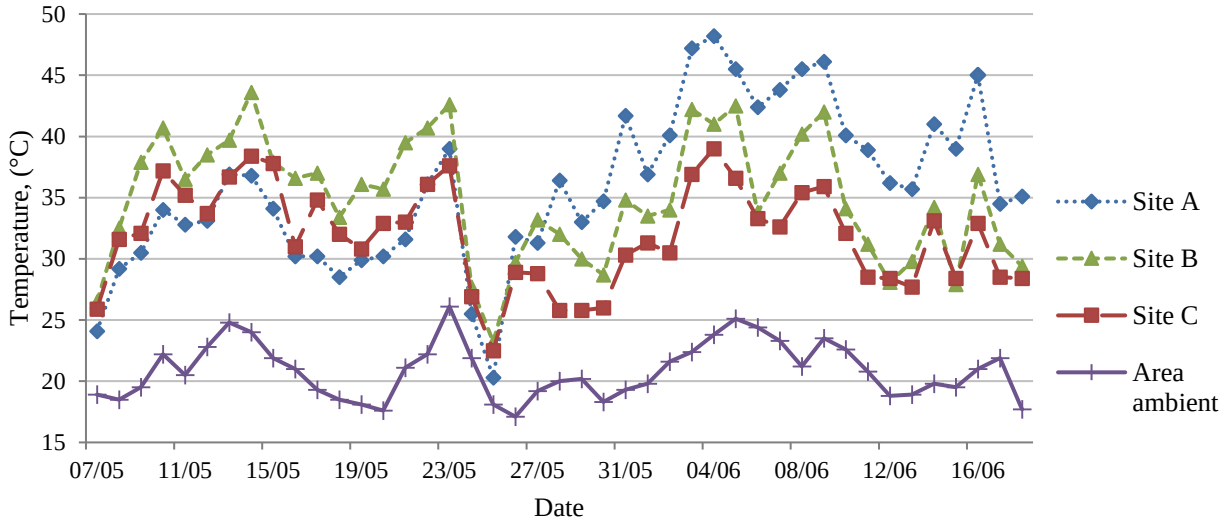

Figure 2 A plot of daily maximum temperature of the 3 active cabinets and ambient air measured in catchment area. The irregular drop on 25/05 was due to a wind and rain. Site A has an irregularity discussed later.

Another piece of information to notice is that after 28/05, the Site A temperature jumped from being the lowest to the highest of the three. The average temperature above ambient before 28/05 was 10.6 °C versus 19.2 °C after, a change of +9.6 °C; this contrasts with Site B and C which had changes of -1.8 °C between the same date ranges.

This 11.4 °C difference was due to a contractor moving the data logger inside the cabinet from the normal place on the rack to a position on top of electronics at the highest point in the cabinet. The rack position was in air temperature one quarter of the height from the top of the cabinet, while the later position was in air at the very top of the cabinet and in contact with electronic components. This inadvertent repositioning demonstrated how the temperature inside a cabinet can differ greatly from an average internal temperature to temperature of air at the top of the cabinet or of a heat producing component.

3.3 Cabinet heat and temperature modelling

The cabinet modelling allows temperatures to be predicted with reasonable accuracy across environments with high heat loads. The model can be used in two approaches; the first can model and predict the probability of a cabinet exceeding threshold temperatures based on historical weather conditions, thereby creating a basis for treatments in the future. An example for a signalised traffic intersection in the North-West of WA is shown below in Table 2.

Probability rating	Likely		Moderate		Extreme	
Ambient temp °C *(chance)*	35	*(0.6)*	38	*(0.3)*	40	*(0.2)*
Wind speed km/h *(chance)*	30	*(0.6)*	25	*(0.3)*	20	*(0.2)*
Solar flux W/m^2 *(chance)*	850	*(0.6)*	900	*(0.4)*	950	*(0.3)*
Cabinet temp °C	40.8		44.9		48.2	

Table 2 Each **c**olumn contains weather conditions for different probabilities and associated cabinet temperature in the bottom row.

The historical weather for the region was analysed from BOM data and three different heat load probability categories established, Likely, Moderate, and Extreme heat loading. The probability for values listed in Table 2 are the likelihood of the environment meeting or exceeding the value listed independently, not necessarily the chance of them all occurring together. The cabinet temperature associated with the conditions in the columns are listed in the bottom row; this sort of analysis demonstrates how the cabinet modelling can be used as a predictive tool for remote regions that can expect high heat loads.

The second approach is to provide an accurate prediction of the temperature of the cabinet with or without heat reduction treatments. For this example, average weather conditions were selected from distant areas across WA, shown on the left of Table 3, and on the right are listed the cabinet temperatures that would correspond to the weather conditions. The temperatures are listed relative to ambient air to standardise the data. This approach can be used to determine whether the time and cost required to install a heat reduction treatment would be worthwhile given the current situation.

Location	Air temp (°C)	Wind speed (km/h)	Solar heat flux (W/m^2)	Normal cabinet (°C)		Heat reflecting paint (°C)		Sunshade (°C)	
Karratha	37.1	20	900	45.5	*+8.4*	40.8	*+3.7*	38.3	*+1.2*
Kalgoorlie	34.5	18.2	1000	44.3	*+9.8*	38.9	*+4.4*	35.7	*+1.2*
Geraldton	32.2	33.0	1000	39.0	*+6.8*	35.2	*+3.0*	33.4	*+1.2*
Bickley	30.7	18.0	1000	40.5	*+9.8*	35.1	*+4.4*	33.4	*+2.7*

Table 3 Left half: rows contain average weather condition for each location. Right half: corresponding temperature predictions for different treatments at each location.

4. Conclusions and Future Work

The aim of investigating heat reduction treatments and creating a model to predict in which environments treatments may be needed and their efficacy has been achieved. As the project progressed, secondary objectives evolved from active cabinet temperature logging, covering finer topics of temperature variation inside cabinets and on exterior surfaces.

Further work to be completed is gathering a statistically significant number of measurements from cabinets' surfaces and installing the three loggers inside cabinets at different elevations as outlined Section 2.2. Future work beyond this project can focus on how heat and temperature vary inside the cabinets; internal geometries and volumes, closed volume natural convection and how air interacts with heat producing components and wall can form a new investigation.

5. Acknowledgements

The author wishes to thank Mr Nathan Lenane of Liquid Protective Coatings for his assistance on specialist coatings and for coating a trial cabinet with Solacoat heat reflective paint coating.

6. References

Chua, H. T. (2019). Thermal performance prediction of outdoor swimming pools. *Building and Environment*.

Delvalle. (2019). Outdoor Encolsures In Desert Areas, Desert Series. In Delvalle (Ed.), (pp. 13). Paso del Prao, Spain.

Hong, Y., Ji, S., Zhai, l., Chen, Q., & Bianco, C. (2008). *Cooling system of outdoor cabinet using underground heat pipe.* Paper presented at the INTELEC 2008 - 2008 IEEE 30th International Telecommunications Energy Conference, 14-18 Sept. 2008, Piscataway, NJ, USA.

Kobayashi, T., Nakamura, M., Ogushi, T., Iwamaru, A., & Fujii, M. (2001). Thermal design of a closed cabinet with a heat exchanger for inner air cooling. *Scripta Technica*, 267-79.

Zhao, J. T., Rao, Z. H., Liu, C. Z., & Li, Y. M. (2016). Experimental investigation on thermal performance of phase change material coupled with closed-loop oscillating heat pipe (PCM/CLOHP) used in thermal management. *Applied Thermal Engineering, 93*, 90-100. doi:10.1016/j.applthermaleng.2015.09.01

The Evaluation of Innovative Technologies for Application to Produced Formation Water Monitoring

Michael Weir

Masoumeh Zargar & Michael Johns
Chemical Engineering
University of Western Australia

Mr. Tim Robertson
CEED Client: Chevron Australia

Abstract

Traditional methods for monitoring produced water are based on 'end of pipe' measurements and include either gravimetric analysis, Infra-Red absorption, or Gas Chromatography and Flame Ionisation Detection (GC-FID). However, despite these being well established and able to provide high precision datasets, the usefulness of the information generated from them is limited and each method has its own drawbacks. With this in mind, this study focusses on sheen detection through the use a remote UV sensor as an alternative produced water monitoring method. In a laboratory environment, this alternative approach showed strong linear trends between sheen detection and the condensate concentration up to 10 minutes after the produced water sample had been created. Furthermore, statistically significant sheens, compared with seawater alone, were detected up to the 20-minute mark. Taking into consideration that produced water production is consistently occurring throughout oil and gas operations, this illustrates that sheen detection is a possible method for detecting the presence of produced water, as well as providing an insight into produced water dispersion and determining the condensate concentration. Hence, these results show that produced water monitoring through the use of remote UV sensors is suitable in laboratory environments.

1. Introduction

1.1. Produced Water

Produced water is derived from fresh and/or brine water that has been trapped, together with oil and gas, in porous sedimentary rock between layers of impermeable rock (Collins 1975). During oil and gas extraction, this entrained water is inevitable extracted (Veil et al. 2004), which is then separated from the oil and gas.

1.2. Produced Water Treatment

Even after the separation process, this water still invariably contains a range of substances, which are potentially harmful to the surrounding ecosystems if released into the ocean (Bothamley 2004). Therefore, it is treated prior to release. Produced water treatment is designed to remove the most volatile hydrocarbons, along with any dispersed non-aqueous liquids, dispersed oil, suspended solids, scale and bacterial particles (Neff and Lee 2011). This process varies from place to place, though at Chevron's Wheatstone platform the treatment process

involves the use of hydrocyclones, gas floatation units and absorption filtration media vessels (Van't Westeinde 2019).

1.3. Produced Water Monitoring

The treatment process, however, can never achieve 100 percent removal and, therefore, there are inevitably trace amounts of contaminants still present afterwards (Neff and Lee 2011). Hence, in order to guarantee that environmenal regulations are met, it is essential that the concentrations of these trace contaminants are continually monitored.

Traditional methods for monitoring produced water are based on 'end of pipe' measurements and include either gravimetric analysis, Infra-Red absorption, or Gas Chromatography and Flame Ionisation Detection (GC-FID) (Neff and Lee 2011). Despite these methods being well established and able to provide high precision datasets, the information generated from them is only for a snapshot in time of a relatively localised area, hence limiting the usefulness of their results. Furthermore, each method has its own draw backs. Infra-Red absorption requires the use of chlorofluorocarbons and, due to their harmful effects to the environment, is being used less frequently, gravimetric analysis is prone to volatile losses, and GC-FID requires sophisticated equipment and skilled operators (Neff and Lee 2011).

1.4. Produced Water Monitoring using Remote Sensors

Due to a combination of temperature and low salinity, the produced water at the Wheatstone platform is strongly buoyant and will move towards the surface soon after being released. This results in it largely remaining in the upper water column and a surface plume forming (Chevron Australia 2016). Hence, with a surface plume forming, it is assumed that a sheen will also form. With this in mind, and combined with their use to monitor oil spills being well documented, an emerging idea is the use of remote sensors for 'sheen detection'. A study on the application of remote sensors was conducted by Chevron (Haselwimmer 2018), with an additional study into the feasibility of using Ultra Violet (UV) sensors for produced water deteciton being conducted as well (Maroef 2019). This later study concluded that, in a laboratory environment, UV sensors are able to detect sheens at the hydrocarbon concentrations associated with produced water, however further analysis was recommended by the researcher.

1.5. Research Objectives

The primary objectives of this study are to expand upon the work of Maroef (2019) and investigate the threshold at which sheen detection begins as well as the relationship between condensate concentration and sheen detectability, in order to determine if sheen detection can provide an insight into the amount of condensate in the water. The secondary and teritiary objective are to determine the effect of time on sheen detection and to better understand the distribution of condensate throughout the water column through the use of a Total Petroleum Hydrocarbon (TPH) analysis, such to provide an insight into the appropriateness of UV sensors.

2. Methodology

2.1. Step 1 – Pre-Laboratory Considerations

Artificial produced water samples were created in the laboratory, of varying condensate-in-water concentrations. A total of 7 concentrations were considered, with 8 samples made for each (Table 1). For each concentration, half of their samples were subjected to 60 minutes of imaging prior to TPH analysis, such to study the effects of concentration and time on sheen development and detectability. The other half underwent TPH analysis immediately after creation, such to compare the differences between the imaging and non-imaging samples, and thus provide an insight into evaporative losses during the imaging process.

Case ID	Condensate Added (µL)	Condensate Added (mg)	Seawater Added (L)	Oil-in-Water Concentration (mg/L)	Imaging Time (minutes)
A	0.0	0.0	0.4	0.00	60
B	1.0	0.78	0.4	1.95	60
C	2.0	1.56	0.4	3.90	60
D	3.0	2.34	0.4	5.85	60
E	4.0	3.12	0.4	7.80	60
F	5.0	3.90	0.4	9.75	60
G	10.0	7.80	0.4	19.50	60
H	0.0	0.00	0.4	0.00	0
I	1.0	0.78	0.4	1.95	0
J	2.0	1.56	0.4	3.90	0
K	3.0	2.34	0.4	5.85	0
L	4.0	3.12	0.4	7.80	0
M	5.0	3.90	0.4	9.75	0
N	10.0	7.80	0.4	19.50	0

Table 1 Experimental Cases Investigated

2.2. Step 2 – Sample Creation

Each sample consisted of 400 mL of seawater, with a micro-pipette being used to measure the required volume of condensate. The seawater and condensate used were taken from UWA's Watermans Bay facility and Chevron's Wheatstone platform, respectively. Clear, 800 mL glass jars with air-tight wooden lids were used to prepare the artificial samples in, with an IKA Mechanical Overhead Stirrer (RW 20 Digital package) with an R 3003 Spiral stirring piece used to create the sample.

2.3. Step 3 – Imaging

A PCO UV camera (Figure 1) and a 50 W TEATRO UV LED floodlight were used during the imaging process. The camera's lens was set to an 'f-stop' of 2.8 and the Camware software settings, as shown in Table 2, were selected. The camera (on its tripod) was situated 0.74 m from the sample, at an angle of 85° below the horizontal. The imaging process was conducted inside a single 210 L container, such that it was void of external light and the light source could be controlled throughout the trials. Furthermore, it was conductwed on a black cloth, using

amber-glass jars. This was done to prevent any light reflecting from the ground as well as to reduce glare caused by the clear-glass jars, hence improving the quality of the images produced.

Parameter	Setting
Exposure Time (ms)	85
Trigger Mode	Auto Sequence
Recording Mode	Sequence
Timestamp	Binary
Allocated # of Images	10

Table 2 Experimental Cases Investigated

Figure 1 PCO UV Camera

Taking into consideration the time for oil droplets to rise from the bottom to the surface of the sample, it was decided that the majority would reach the surface by the 15-minute mark, with the vast majority reaching the surface by the 60-minute mark. Hence, 1-minute imaging intervals were conducted from the 5-minute to the 15-minute mark to provide an insight into the sheen formation during this period of time, with imaging being continued until the 60-minute mark at 10-minute intervals, after which it was concluded that sheen formation was no longer occurring.

2.4. Step 4 – TPH Analysis

Once the imaging process was complete, the sample was separated into top and bottom halves (200 mL each) with 15 mL of cyclohexane being added to each, such to extract the condensate from the seawater. Pasteur pipettes were then used to extract the cyclohexane-condensate layers. To perform the TPH analysis, an ERACHECK PRO machine was utilized. This machine is capable of measuring the concentration of condensate within cyclohexane, hence allowing for the concentration of condensate in the sample to be calculated.

2.5. Step 5 – Image Analysis

The image analysis was conducted using ImageJ, an open source Java-based imaging process program. It was used to perform a flat field correction on each of the images, threshold the images and then calculate the relative sheen intensity.

3. Results and Discussion (Imaging)

For each trial, the average relative sheen intensity (ARSI) was taken as the average of the 10 images' relative sheen intensities at each point in time. For each experimental condition, the overall mean relative sheen intensity (OMRSI) at each point in time was calculated as the average of its respective ARSIs.

Even after thresholding, there was still a very slight sheen detected in the Experiment A trials, despite no condensate being added. Therefore, any sheen being produced here was attributed to reflection from the seawater. A two standard deviation increase was applied to each OMRSI from Experiment A, with the largest value of these taken as the 'background sheen'. Hence, OMRSIs were required to be greater than this in order to be considered a sheen associated with the presence of condensate.

The OMRSIs obtained indicate that the UV sensor is able to detect a sheen greater than the 'background sheen' at least 50-minutes after the condensate has reached the surface of the sample.

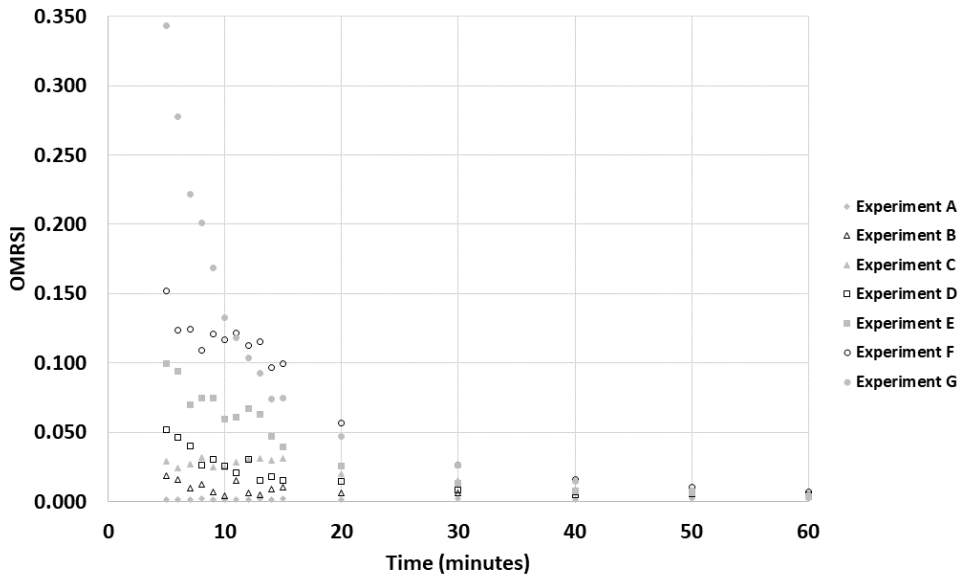

Figure 2 Overall Mean Relative Sheen Intensity vs. Time

As seen in Figure 2, the OMRSI decreases at a decaying rate, with it decreasing rapidly initially before approaching a plateau over time. This would indicate that within the first 5-minutes, the majority of sheen formation has occurred and that, after this, evaporation is the dominating factor. Furthermore, with there being differing quantities of condensate between experiments as well as condensate decreasing over time, this would explain the differing decay rates between experiments.

4. Conclusion and Future Work

The detection threshold at which the UV sensor was unable to detect a statistically significant sheen at the 5-minute mark was not found. However, it is clear that, with an increase in concentration, there is an increase in the sheen produced, particularly within the first 10 minutes of imaging. Furthermore, at the 5-minute mark, the OMRSIs detected by the UV sensor were statistically significant compared with each other. Therefore, in a laboratory environment, it is possible to use a UV camera to provide an insight into the oil-in-water concentration at the 5-minute mark.

However, sheen detectability decreased at a decaying rate over time, with it initially decreasing rapidly before approaching a plateau over time. This resulted in the sheen detected quickly being no longer statistically significant between experiments after the 20-minute mark. Hence, for the concentrations investigated in this study, the use of UV sensors for determining the concentration based of sheen detectability over time periods much greater than 20-minutes is not suitable.

Taking into consideration that the produced water treatment process is constantly operating during the oil and gas process at the Wheatstone platform, produced water production is likely to be constant. With this in mind, it is likely that any condensate lost to evaporation will be replaced by new produced water rising to the surface. Hence, issues associated with sheen detection reducing over time in the laboratory may not be issues in the real world.

5. Acknowledgements

I would like to thank the following people for their assistance throughout this project:
- Dr. Jeremy Leggoe and Ms. Amanda Bolt for organising the CEED program.
- Dr. Nicholas Ling for his assistance and advice in the laboratory.
- Mr. Andrew Van de Ven for supplying the seawater samples.
- Mr. Jonathan Brant and Mr. Andrew Parton for inspection and repairs to the UV Floodlight.
- Mr. Dzyan Maroef for his continuous advice and guidance throughout the project.

6. References

Bothamley, M 2004, 'Offshore processing options vary widely', *Oil & Gas Journal*, vol. 201, no. 45, pp. 47-55

Collins, A 1975, *Geochemistry of Oilfield Waters*, Elsevier Scientific Publishing Company, New York.

Chevron Australia. (2016) *Wheatstone Project Start Up and Operations Environment Plan Summary*. Internal Chevron report. Unpublished.

Haselwimmer, C. (2018) *Review of Remote Sensing Approaches for Wheatstone PWD Monitoring*. Internal Chevron report. Unpublished.

Maroef, D 2019. 'Produced Water Remote Monitoring'. Masters these, Univeristy of Western Australia, Perth.

Neff, J & Lee, K 2011, *Produced Water: Overview of Composition, Fates, and Effects*, Springer, New York.

Van't Westeinde, P. (2019). *Wheatstone Upstream 1645 Produced Water Treatment System Operating Manual, Volume 1 – Process and Equipment Description*. Internal Chevron report. Unpublished.

Veil, J.A, Puder, M.G, Elcock, D & Redweik R.J 2004. *A white paper describing produced water from production of crude oil, natural gas, and coal bed methane*, Argonne National Laboratory, Lemont

Produced Water Remote Monitoring

Alexander Tan

Charitha Pattiaratchi
Oceans Graduate School & The UWA Oceans Institute
The University of Western Australia

Tim Robertson
CEED Client: Chevron

Abstract

There is opportunity to improve the management of Produced Formation Water discharges from offshore oil and gas facilities through remote monitoring. As a global leader, Chevron seeks to pave the way through the investigation of the latest sensor technology to accomplish this. Remote monitoring has the potential to remedy drawbacks of current processes such as the reliance on end of pipe wet chemistry data and intensive vessel-based campaigns. These methods carry high-risk and are financially demanding. With developments in sensor technology, there is significant potential to refine and build both feasibility and robustness into Produced Formation Water monitoring processes.

This project investigates the performance and limitations of in-situ fluorometers through bench-testing and field-testing. Five in-situ fluorometers on the market have been considered. Parameters, particularly sensitivity and lower limits of detection, will be investigated with samples including Produced Formation Water sourced from Chevron facilities.

Outputs of the project include a bench-testing and field-testing report in addition to a final detailed report that contrasts the performance of the sensors. The conclusions will evaluate the feasibility of the sensors for field implementation.

1. Introduction

The current methods for monitoring Produced Formation Water (PFW) have limitations including, but not limited to, costly and high-risk vessel-based field campaigns, use of chemical additives, and a lack of access to real-time data (Kato et al., 2017). Methods rely heavily on "end of pipe" wet chemistry data which are resource intensive to process, and numerical modelling which is extrapolatory in nature for ongoing operations and relies upon field validation via vessel campaign. An alternative remote monitoring process has the potential to significantly cut back on these costs and resources. However, there is limited literature and industry examples available at present to support large scale implementation. The potential benefits of remote sensor technologies in the market at present have prompted this project. In order to be applicable in offshore oil and gas (O&G) operations, further research and testing into the capabilities and compatibilities of in-situ fluorometers is required. The adoption of remote monitoring methods has the potential to address the aforementioned issues as well as better evaluate plume propagation and monitor impacts.

Remote monitoring sensor technologies potentially provide an opportunity to more efficiently conduct data collection, enabling better evaluation of hydrocarbon plumes as they propagate away from the point of discharge. The majority of these sensors are submersible and utilise fluorometry in determining various hydrocarbon concentrations, and are as such, classified in-situ fluorometers. The capabilities and limitations of many of these sensors including, but not limited to, the Sea-Bird Scientific SeaOWL UV-A, Turner C3 Submersible Fluorometer, Chelsea Technologies UviLux Fluorometer, and TriOS EnviroFlu-HC were investigated by an EU Horizon 2020 funded group known as the GRACE Project (Pärt & Kõuts, 2016).

In collaboration with research organisations such as UWA, Chevron seeks to evaluate the latest sensor technology with a view to incorporate in-situ fluorometers to PFW analysis processes. This project has multiple drivers beyond financial including seeking to improve environmental outcomes via direct measurement in the marine environment, rather than relying upon end of pipe data, and predictive models to extrapolate. There is potential to improve the safety of the process and minimise the risk to employees through remote sensor operation. Further, reducing the need for vessel operations aligns with initiatives such as the Paris Agreement (Rogelj, et al., 2016) which are motivating resource industry leaders to adopt lower carbon emission methods.

2. Project Execution and Experimental Design

2.1 Experimental Design

The practical component of the project is being executed in three phases, calibrations, preliminary testing, and trials. With each sensor having unique methods of calibration and accommodating software, each sensor required initial setup and familiarisation took time.

The second phase involved conducting preliminary tests for each sensor to ensure that each could perform adequately under a common experimental setup to control the trials as much as possible. These tests included analysing interferences on sensor performance and are detailed as follows:

- Container edge effects - Sensors are tested at various distances from the edge of a black plastic container. Following this, the minimum distance from the container bottom was determined by testing the sensors at various distances from the bottom. The minimum distance is deemed to be the point at which channel values plateau.
- Ambient light – Sensors are trialled in three different environments, enclosed with no light, laboratory lighting, and outside under sunlight.
- Solution movement – Magnetic stirrers are utilised in samples to maintain a degree of solution homogeneity and investigate whether significant solution movement interferes with sensor readings.

Additionally, the sample was tested to investigate appropriate handling and storing methods. The sample stability was tested over time by taking measurements at fixed intervals over one week. PFW samples are also tested at a variety of temperatures using the sensors to determine if temperature control is required.

In the final experimental phase, a range of PFW dilutions are trialled, particularly at the low concentration range. Trials are conducted with five replicas to gauge the reliability of results and average performance. The range of samples is being informed by previous studies and cross-referenced with the stated specifications of the sensors. The limit of detection and

reliability for each sensor to detect changes TPH concentration is also being investigated. The necessary blanks with distilled water in addition to dilutions with other influences of either chlorophyll or seawater are also tested. Introducing chlorophyll and seawater allows for the samples to better resemble water conditions near offshore facilities and assess the robustness of the sensors in the presence of background interference from non-target constituents.

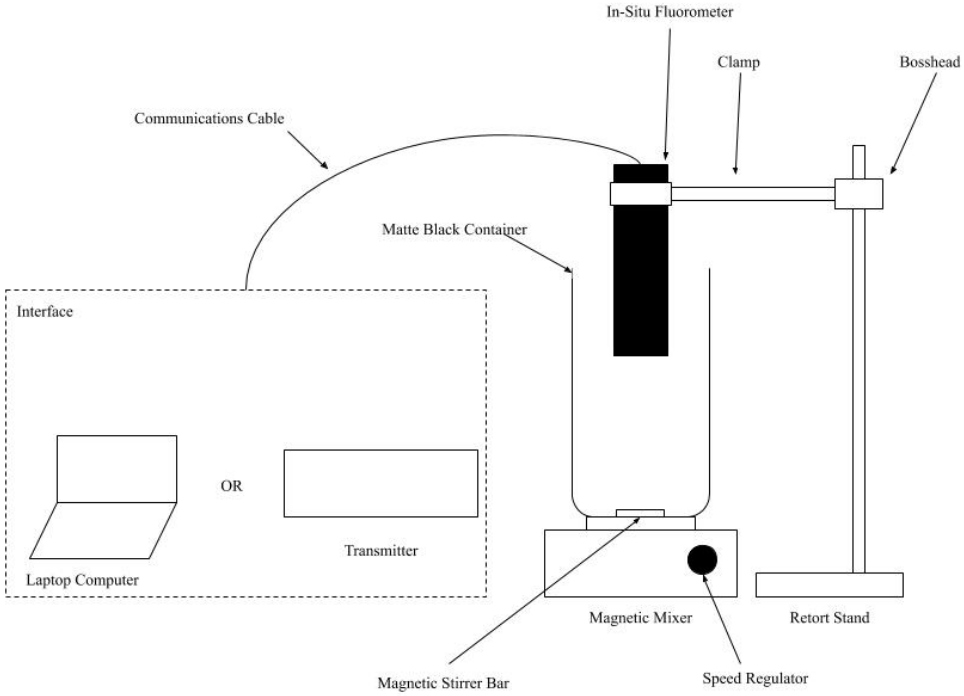

Figure 1 Experimental apparatus for Produced Formation Water trials.

Figure 1 captures the general experimental apparatus for the sample trials. The sample is hosted on a magnetic stirrer device in a matte black cylindrical container. The sensor is held above by clamps and a retort stand whilst connected to the required interface. Sensors are submerged approximately 2cm during testing.

2.2 Feasibility Study

Should the results of bench-testing be sufficient to warrant a field-test, research into the feasibility of implementing the sensors will be conducted. This will include a literature review into unmanned or remote operable technologies that are able to host the sensors.

3. Results and Discussion

Three sensors have been analysed to date for user friendliness and compatibility in regard to setup processes, build robustness, data processing. These sensors will be designated sensors A, B, and C. Further, preliminary tests were conducted on each sensor to determine their sensitivity to potential physical interferences in the bench-testing space.

3.1 Setup

Sensor A and B require installation of drivers and software. Following this the parameters such as the bitrate need to be set. The communication cables and separate power cables are then attached. Sensor C is available with a transmitter. The transmitter is an external unit that can process the data in an already pre-set interface.

3.2 Build Robustness

Sensors A and C are of similar size and robust-type build. The electronics are completely contained in housing with dimensions of 28cm length by 6.3 cm diameter and 31cm length by 6.8cm diameter respectively. Sensor B is a much more compact unit and was not provided with a waterproof housing however, this option is available. It stands at 4.1cm height and 7.7cm diameter.

3.3 Data Processing

Sensor B differed from the other two with the software not being able to provide a live graphical representation of the data. The feed from the sensor was provided numerically at a refresh rate of approximately 1-2 seconds. In contrast the other two sensors were complimented with much more modern interfaces which provided graphical interpretations of data. The refresh rate of Sensor C however, did prove to be significantly slower than the other two sensors at approximately five seconds in the fastest case.

3.4 Initial Tests

The preliminary tests for each sensor are designed to determine whether each could perform adequately under the experimental setup allowing for as much experimental control as possible. These tests included analysing interferences on sensor performance and are detailed as follows:

- Container edge effects - Sensors are tested at various distances from the edge of a black plastic container. Following this, the minimum distance from the container bottom was determined by testing the sensors at various distances from the bottom. The minimum distance is deemed to be the point at which channel values plateau.
- Ambient light – Sensors are trialled in three different environments, enclosed with no light, laboratory lighting, and outside under sunlight.
- Solution movement – Magnetic stirrers are utilised in samples to maintain a degree of solution homogeneity and investigate whether significant solution movement interferes with sensor readings.

Additionally, the sample was tested to investigate appropriate handling and storing methods. The sample stability was tested over time by taking measurements at fixed intervals over one week. PFW samples are also tested at a variety of temperatures using the sensors to determine whether temperature control is required. The PFW samples showed negligible degeneration in quality over time, which is expected as the samples have been in storage for approximately one year prior.

Table 1 describes the performance of the available sensors in the preliminary tests.

Sensor	Container Edge Effects	Ambient Light	Solution Movement
A	Negligible interference when perpendicular Minimum measurement distance: 11cm	Negligible	Negligible
B	Negligible interference when perpendicular Minimum measurement distance: 8cm	Negligible	Feed occasionally flatlines for a short period or until sensor is removed and submerged again.
C	Negligible interference when perpendicular Minimum measurement distance: 10cm	Negligible	Experiences slight shift in feed of $\pm$(1-2) μg/L

Table 1. Preliminary tests summary table

4. Conclusions and Future Work

The results of the preliminary tests have been deemed satisfactory to proceed with PFW trials. The performance of the sensors, particularly Sensor B, in regard to solution movement will continue to be analysed throughout the PFW trials utilising the results of the ERACheck Pro, an oil-in-water measurement device, as a point of reference.

Currently, PFW dilutions are being made and cross-checked with the ERACheck Pro. Refinements are being conducted to clarify the dilution methodology. Once the dilution methodology is satisfactory, first the distilled water and PFW trials will be conducted, followed by the seawater and PFW trials, with the chlorophyll spiked distilled water and PFW trials last. At the moment two in-situ fluorometers, Sensor D and E, are not available. Should these become available, calibrations and preliminary tests will also be conducted for these sensors.

Pending the results of the project, field test validation of those sensors which perform satisfactorily need to be conducted. Should time allow, small scale field-tests will be conducted, however, ultimately the goal is to have the sensors hosted in an unmanned vehicle that is capable of remote operation from an offshore facility.

5. Acknowledgements

Additional acknowledgements are extended to the following individuals external to the primary project team. Dr. Brendan Graham and Prof. Michael Johns for providing laboratory space and the ERACheck Pro for use. Dr. Graham’s insights and experience with PFW samples has also been helpful in refining experimental methods. Fellow CEED scholar Michael Weir for his explanation of methods utilised in a similar project and insights into utilising the samples in bench-tests.

6. References

Kato et al. (2017). An autonomous underwater robot for tracking and monitoring of subsea plumes after oil spills and gas leaks from seafloor. *Journal of Loss Prevention in the Process Industries, 50*(B), 386-396.

Pärt, S., & Kõuts, T. (2016). *In-situ oil detection sensor – technology overview and experiment design.* Tallinn.

Rogelj, J., den Elzen, M., Höhne, N., Fransen, T., Fekete, H., Winkler, H., . . . Meinshausen, M. (2016). Paris Agreement climate proposals need a boost to keep warming well below 2°C. *Nature*, 631-639.